Temporal Correlations Between External Gravitational Geometries and Relevant Geophysical Phenomena in the Campi Flegrei–Vesuvio Volcanic Area

Adriano Ballabene [1]

[1] *Raffaele Bendandi House Museum and Municipal Geophysical Observatory, Faenza, Ravenna*
(affiliate and honorary member, independent researcher, software developer)

Abstract

The Campi Flegrei caldera, located west of Naples, is affected by slow vertical ground deformation, with maximum uplift centered in the Rione Terra area of Pozzuoli. Since 1905, six major uplift phases have been recorded, suggesting some degree of periodicity in the deformation process. However, this periodicity is irregular, owing to pronounced variations in the rate, duration, and associated seismicity of individual episodes (Fig. 1).
The mid-points of subsidence phases exhibit a relatively regular frequency; however, the existence of a true cyclicity in the bradyseismic phenomenon cannot be confirmed. This is due both to the anomaly represented by the 1982–1984 interval, which occurred at least three years out of phase with respect to the expected trend, and to the complete incongruence of the 2009–2021 interval, characterized by slow ground uplift during a period in which, by recurrence, subsidence would have been expected (Fig. 2).
Excluding these major and prolonged discrepancies, as well as shorter ones—likely attributable, at least up to the post-war period, to insufficient measurement frequency—a correlation can be observed between bradyseism and the lunar transit altitude in the local celestial sphere:

Periods with lunar culminations $< 75°$ → Subsidence (Fig. 3)
Periods with lunar culminations $\geq 75°$ → Uplift (Fig. 4)

The analysis, which also aimed to interpret the discrepancies observed in the two main correlations, was conducted using three distinct approaches, sharing the use of lunar orbital parameters and high geometric accuracy. This accuracy was obtained by segmenting the lunar distance into five intervals and applying different levels of angular precision. Overall, the study reveals significant temporal coincidences between specific geometric configurations of the three main external gravitational sources acting on the Earth system and major geophysical phenomena recorded in the Campi Flegrei–Vesuvio volcanic area. These include: (i) the multi-year phases of vertical deformation, both periodic and aperiodic; (ii) the main inconsistencies with respect to such phases, (iii) the historical eruptive events (AD 79, 1302, 1538), (iv) the seismic crises of 1982–1984 and 2022–2025, (v) the short uplift episodes of 1976, 1989, 2000, 2005, and 2012, (vi) the major earthquake of 1883, seismic shocks of uncertain correlation in AD 37 and 1199, and some of the aforementioned events, such as those of 1302, 1976, and 2025.

1 Introduction

Overall, the subsidence-to-uplift transition phases (1907–1913, 1928–1933, and 2005–2006), the acceleration phases of uplift (1950–1952, 1968–1972, and 1982–1984), and the seismic crises (1983–1984 and 2022–2025) suggest a periodic pattern (Fig. 4). This recurrence is irregular, however, due to variations in the duration, rate, and seismicity of individual deformation phases. The pattern is further disrupted by the 1982–1984 interval, which occurred at least three years out of phase (Point 1, Fig. 2), and by anomalous periods such as the slow uplift of 2009–2021 (when subsidence would have been expected; Point 2, Fig. 2) and the subsidence of 1985–1990 (Point 3, Fig. 2).
The mid-points of the subsidence phases display a more regular frequency. In most cases, descending bradyseismic phases coincide with periods when lunar culminations remain consistently below 75° (Fig. 3), with durations of ~12.1 years and recurrences of ~6.5 years. Conversely, uplift phases (Fig. 4) correspond to intervals of about 6.5 years, recurring every ~12.1 years, during which lunar culminations exceed 75° for 1–4 days per month.

The pair of intervals of 12.1 and 6.5 years corresponds to a subdivision of the lunar nodal (draconic) cycle of 18.6 years, a pair that occurs in Pozzuoli as in any other locality at the same geographic latitude (40.83° N). The main inconsistencies of the two correlations — |Periods of lunar culminations < 75°| → |Subsidence| and |Periods of lunar culminations ≥ 75°| → |Ground uplift| — are consistently interpreted through additional analyses, based on two distinct approaches but sharing the evaluation of lunar orbital parameters (both local and geocentric–equatorial) and a high degree of geometric accuracy. While the first approach is limited to the analysis of the Moon alone and of a single parameter, namely its local height above the horizon of Pozzuoli (thus ignoring the Earth-Moon distance and the lunar phase of the Moon between Earth and the Sun), the second, more detailed and methodologically refined, also considers the Sun but only during the New Moon phase and is based on a segmentation of the lunar distance into three specific Perigee intervals, on a zeroed measurement in the identification of the culmination and on the subdivision into two distinct bands of the angular distance between the exact syzygial alignment (calculated with respect to the equatorial axis, i.e. in a geocentric-equatorial reference system and not only geocentric, i.e. in Right Ascension) and the meridian passing through Pozzuoli. The geometric accuracy thus achieved has made it possible to identify specific correlations between the most relevant luni-solar configurations - characterised by an enhancement of the gravitational forcing - and the main paroxysmal events in the Campi Flegrei-Vesuvius volcanic arc, including the uplift episodes—and the major paroxysmal events in the Campi Flegrei–Vesuvius volcanic arc, including uplift episodes (short-term, multi-year periodic, the out-of-phase event of 1982–1984 and the apparently incongruent period 2005–2021), the major seismic shocks and some of the most significant eruptions such as those of 79 AD, 1302 and 1538. The analysis shows how Jupiter, at very close angular distances from the close Moon-Sun conjunctions, was configured shortly before the last eruption in Ischia (1302 AD), the Casamicciola earthquake (Mw 4.2, 1883), the Vesuvius eruption of 1906, the marked acceleration of uplift likely dating to 1976, and the Md 4.6 earthquake of 30 June 2025 — the strongest bradyseismic shock at Campi Flegrei since at least 1584, together with that of 13 March 2025.

Overall, the study does not adhere to a rigorous statistical methodology: the lack of a significant portion of essential measurements prior to 1950, and the absence of daily records before the 1980s, would compromise the reliability of any correlation analysis. The analysis does not allow for consistent and uniform statistical validation of the correlation between various kinds of astronomical configurations and heterogeneous geophysical phenomena.

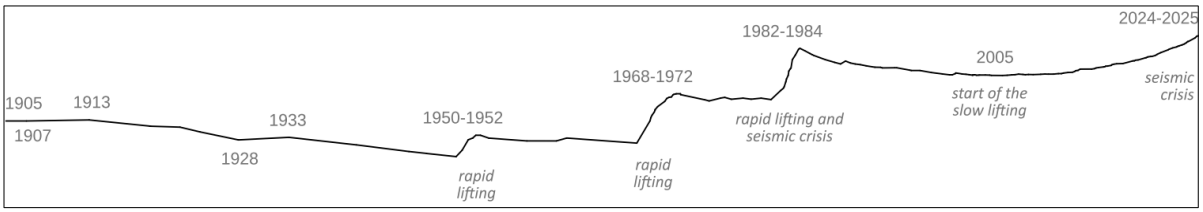

Fig. 1 The Bradyseismic Activity at the Phlegraean Fields from 1905 to 30 June 2025.

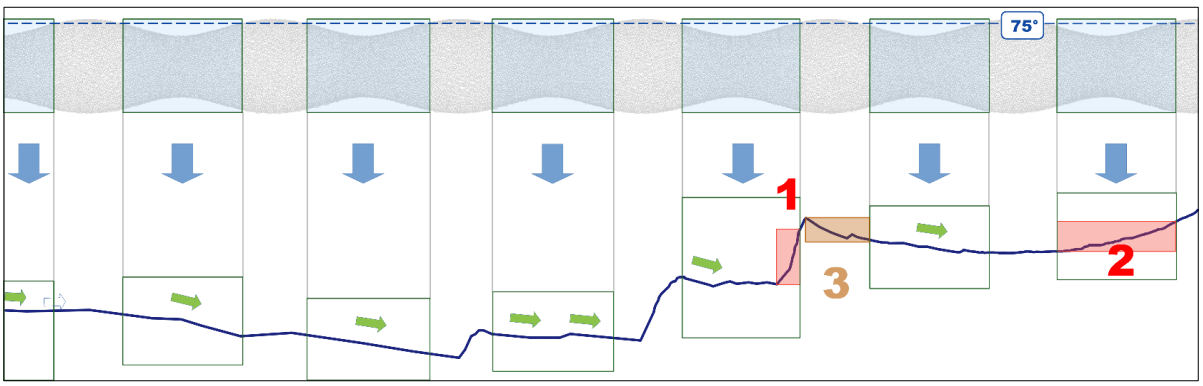

Fig. 2 1905–30 June 2025. Points 1 and 2 highlight inconsistencies between periods of lunar culminations with altitudes always below 75° (boxed and shaded at the top) and the subsidence of the ground, indicated by the downward green arrows. Point 3 highlights an inconsistency between a period with culminations exceeding 75° in altitude and a phase of ground lowering.

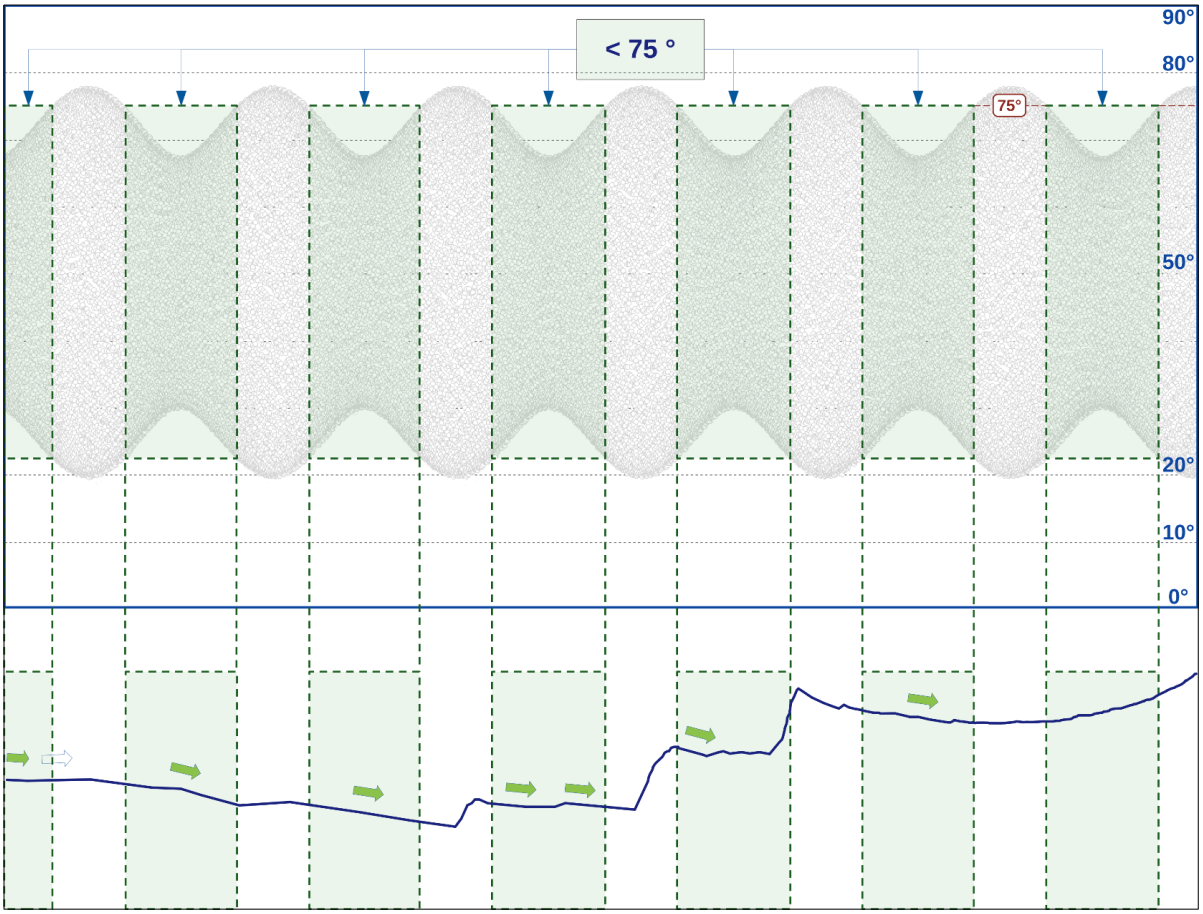

Fig. 3 Period 1905–30 June 2025. Concurrences between most phases of Phlegraean ground subsidence (bottom) and the periodic geometric phases of lunar culminations with local altitude consistently < 75° (top), boxed and shaded in green.

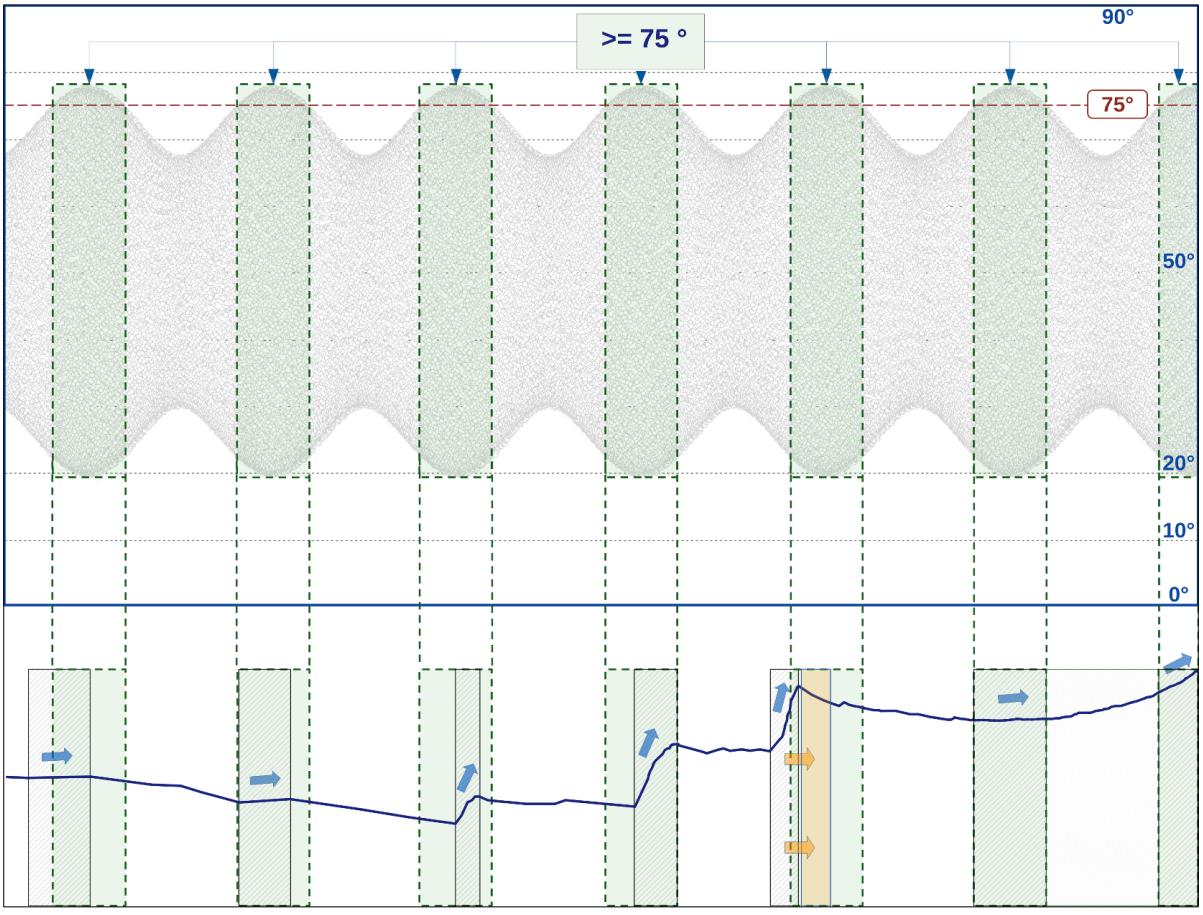

Fig. 4 Period 1905–30 June 2025. Concurrences between most phases of Phlegraean ground uplift (bottom) and the periodic geometric phases with lunar culminations of local altitude ≥ 75° (top), boxed and shaded in green.

2 Data, analysis, results, calculation method

2.1 Data Sources

- Astronomical coordinates. Generated with the astronomical simulation software Solex (Solar System Integration by a Fast Extrapolation Method), developed by Prof. Aldo Vitagliano, University of Naples Federico II.
- Figures and plots. Unless otherwise attributed, all graphics (figures, plots, diagrams) were produced by the author using Microsoft development tools.
- Visual verification. All significant configurations were visually verified with Solar System Simulator Studio, version 1.1.6 (2004–2006).
- Seismicity. Seismic data for the Neapolitan area were obtained from the Osservatorio Vesuviano of the Istituto Nazionale di Geofisica e Vulcanologia (INGV) through the official portal.
- Ground deformation. Records of Phlegraean ground deformation are derived from INGV publications, including the Bollettino dell'Osservatorio Vesuviano.

2.2 Temporal Correlations between Culminations and Vertical Ground Deformation

2.2.1 Graphical Representation of the Moon

The extended harmonic in Figs. 3–4, within the frame representing the celestial sphere of Pozzuoli, graduated on the right with angular heights relative to the local horizon, consists of 44011 gray disks, each representing the Moon at its maximum angular height (culmination) reached on each day of the period 1 January 1905–30 June 2025.

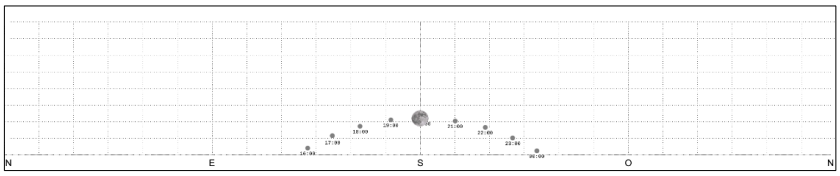

Fig. 5 The lunar position in the celestial sphere of Pozzuoli at each hour on 4 September 1984. The culmination, at the center of the celestial sphere and on the local meridian (S), reached an altitude of 22.10° above the local horizon.

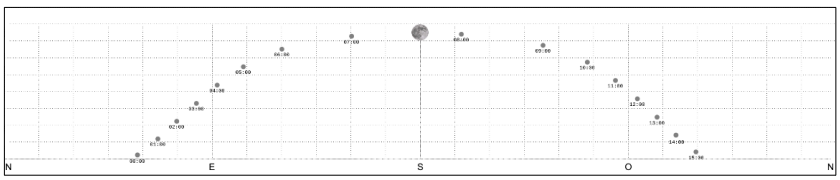

Fig. 6 The lunar position in the celestial sphere of Pozzuoli at each hour on 20 September 1984. The culmination, at the center of the celestial sphere and on the local meridian (S), reached 74.68° above the local horizon.

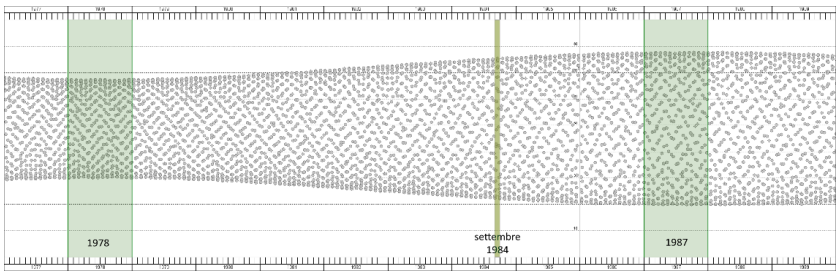

Fig. 7 Period 1977–1989. The time series of lunar culminations at Pozzuoli. The graph corresponds to a portion (the scale on the altitude axis has been reduced for graphical reasons) of the representation shown in Figs. 3–4, limited to the period 1977–1989. The generic years 1978 and 1987 and the month of September 1984 are highlighted. At the latitude of Pozzuoli (40.83° N), the Moon culminates daily at an altitude ranging between 20.6° and 77.8°. At latitudes lower than about 66.5° worldwide, the Moon rises and sets every day, thus remaining visible during at least part of the diurnal cycle.

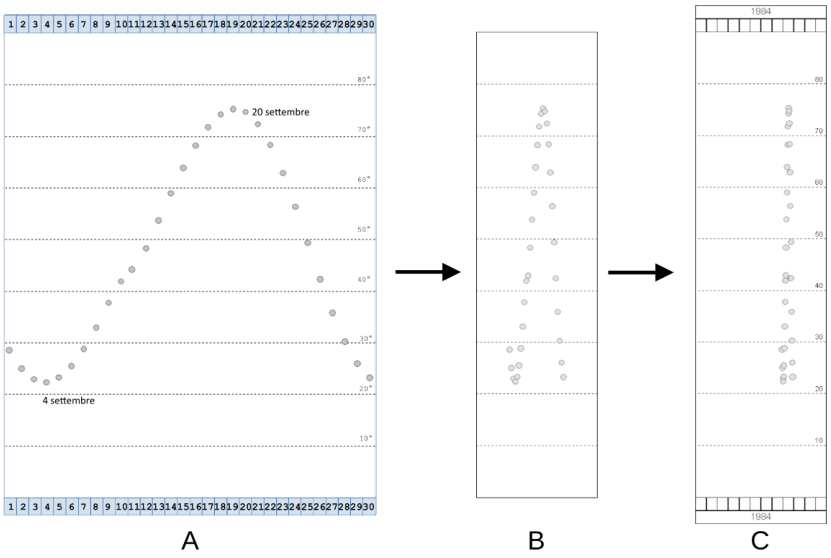

Fig. 8 Local culminations of September 1984, displayed with increasing graphic density (compressed in Fig. 7).

Figs. 5 and 6 illustrate the lunar positions in the celestial sphere of Pozzuoli at each hour on 4 and 20 September 1984, including, at the center of the frame, the two culminations. Figs. 8A–C, 2, 3, 4, and 7 show lunar culminations only. Figs. 8A–C are displayed with progressively increasing graphic density, in order to allow visualization within a more compact space.

2.2.2 Analysis of the angular distribution of lunar presence in the local celestial sphere

The plots shown in Figs. 9 and 10 display, with reference to the local horizon of Pozzuoli, the hourly positions of the Moon for the years 1978 and 1987, selected as illustrative examples (highlighted in Fig. 7). Years with lunar culminations reaching altitudes ≥ 75 degrees (e.g., 1987) are characterized by a wider distribution of the Moon in the celestial sphere, compared to years such as 1978, when culminations remained consistently below 75 degrees (specifically < 68°).

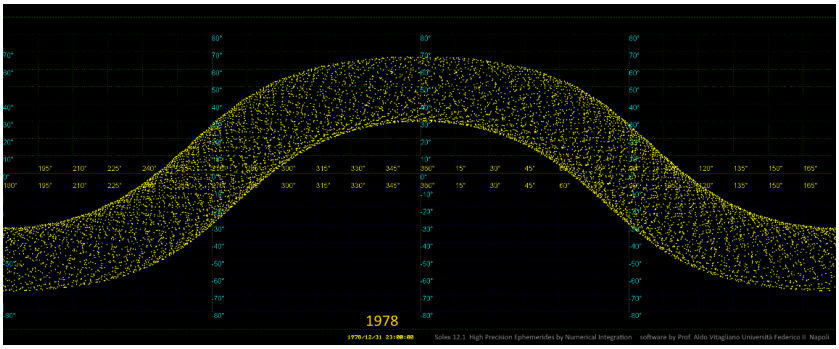

Fig. 9 The lunar positions at each hour of the year 1978 (a year with lunar culminations always below 75°).

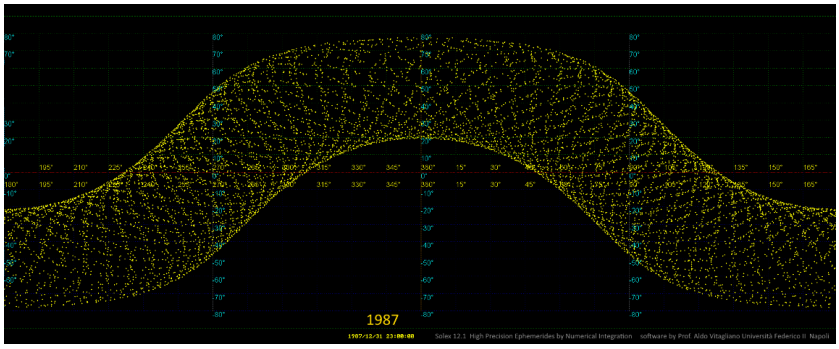

Fig. 10 The lunar positions at each hour of the year 1987 (a year with lunar culminations exceeding 75°).

2.2.3 Temporal Correlations between Culminations and Vertical Ground Deformation

The analysis does not include the calculation of gravitational factors nor the direct evaluation of geophysical parameters; instead, it considers predominantly geometric elements. The study adopts an exploratory approach, and the results can be interpreted solely through the graphical outputs and tabulated data generated by the Solex software. The research is structured in three complementary phases. Each phase, considered in isolation, does not allow for statistical validation of the correlation between heterogeneous geophysical phenomena and astronomical configurations of distinct categories.

The first approach, which is limited to considering only the local altitude of the lunar orbit, is more elementary in nature than the subsequent one. The initial partial results can be assessed in the graphs presented in Figs. 3–4. The analysis does not follow a rigorous statistical methodology: the absence of a significant portion of essential measurements prior to 1950 and of daily data before the 1980s would compromise the validity and reliability of a correlation analysis.

The intrinsic complexity and dynamic nature of deep magmatic processes, which are not directly observable, further hinder a comprehensive evaluation, since the surface manifestations of their effects do not necessarily follow a direct or linear causal relationship. Although the correlations obtained in the preliminary phase of the analysis were not fully conclusive, they nonetheless highlighted elements of sufficient interest to justify further investigation. In this context, the analysis was extended to include additional astronomical parameters, such as the Earth–Moon geocentric distance, the conjunction of the Moon with the Sun, and the angular or temporal distance between the syzygial culmination and the local meridian of Pozzuoli.

2.3 Temporal Correlations among Moons at Minimum, Super, and Extreme Perigee (including both Daily Culminations and New Moons), Major Volcanic Eruptions, and Periodic and Aperiodic Ground Uplift

2.3.1 Graphical Representation of the Moon

The subdivision of the lunar perigee into three main bands — with particular attention to those perigees coinciding with New Moon culminations — provides an interpretative framework useful for clarifying some of the inconsistencies observed in the correlation between Phlegraean bradyseism dynamics and the lunar transit altitude recorded at Pozzuoli. This approach also highlights significant relationships between the geometrically most attractive luni-solar configurations and some of the major eruptions that occurred in the Campi Flegrei–Vesuvius volcanic district, such as those of AD 79, 1302, and 1538. Fig. 11 shows the classification of lunar culminations, represented as colored disks according to the Earth–Moon distance[1]. Fig. 12 instead illustrates the classification of New Moons, represented as chromatically distinct spheres corresponding to the following orbital conditions: Extreme Perigee, Super Perigee[2], Minimum Perigee, Intermediate Distance, and Apogee.

Extreme perigee culmination	< 357400 km
Super perigee culmination	≥ 357400 & < 359600 km
Minimum perigee culmination	≥ 359600 & < 373500 km
Intermediate distance culmination	≥ 373500 & < 390000 km
Apogee culmination	≥ 390000 km

Fig. 11 Classification of Lunar Culminations according to the Earth–Moon distance.

Fig. 12 New Moon at Extreme Perigee (red), at Super Perigee , at Minimum Perigee, at Intermediate Distance, and at Apogee.

1 In the diagrams reported in Figs. 2–10, the Moon is represented with constant size and chromaticity, since no additional orbital parameters were incorporated into the graphical model.

2 Moons at Super Perigee (represented by an orange disk in the figures), regardless of their phase, as well as New Moons at Super Perigee occurring in an Earth–Moon–Sun alignment (represented by a cobalt-blue sphere), must be distinguished from the journalistic Supermoons. The latter correspond to Full Moons at distances shorter than 360 000 km, which occur in a Moon–Earth–Sun configuration rather than in an Earth–Moon–Sun alignment.

2.3.2 Analysis of historical periods

The most significant inconsistencies in the correspondence |Lunar culminations < 75° → Descending bradyseism| (highlighted by the red boxes in Fig. 2 and referring to the 1982–1984 bradyseismic crisis and to the 2009–2021 interval of the current ascending phase) cannot be resolved by considering solely the local altitude of the lunar orbit.

The gravitational effect exerted by the Moon on the Earth's surface reaches its maximum under orbital and geometric configurations in which three fundamental conditions combine:

- Maximum altitude above the horizon – the Moon is at its minimum zenith distance, resulting in an increased vertical component of the gravitational force;
- Perigee – the Earth–Moon distance is minimal; compared to apogee, the gravitational attraction can increase by up to ~20%;
- New Moon (syzygy) – the Earth–Moon–Sun alignment produces the vector sum of lunar and solar gravitational forces, with an amplifying effect.

Although independent, these three parameters exhibit harmonic variations, with multiples or fractions of fundamental cycles evolving on different temporal scales. The resulting oscillations generate maxima that may occur at distinct times—due to their independence—or, occasionally, in temporal coincidence. In both cases, whether individually or combined, the gravitational peaks develop gradually.

The variation in lunar gravitational attraction is thus governed by continuously evolving orbital and geometric conditions:

- lunar declination varies according to the nodal precession (~18.6 years), progressively modifying the maximum altitude achievable above the local horizon;
- the geocentric distance evolves regularly along the elliptical orbit, leading gradually to perigee and subsequently to apogee, with an additional modulation imposed by the rotation of the line of apsides (~8.85 years) [3] ;
- the synodic cycle (~29.53 days) defines the progression toward syzygy, where the additive contribution of the solar gravitational component is maximized.

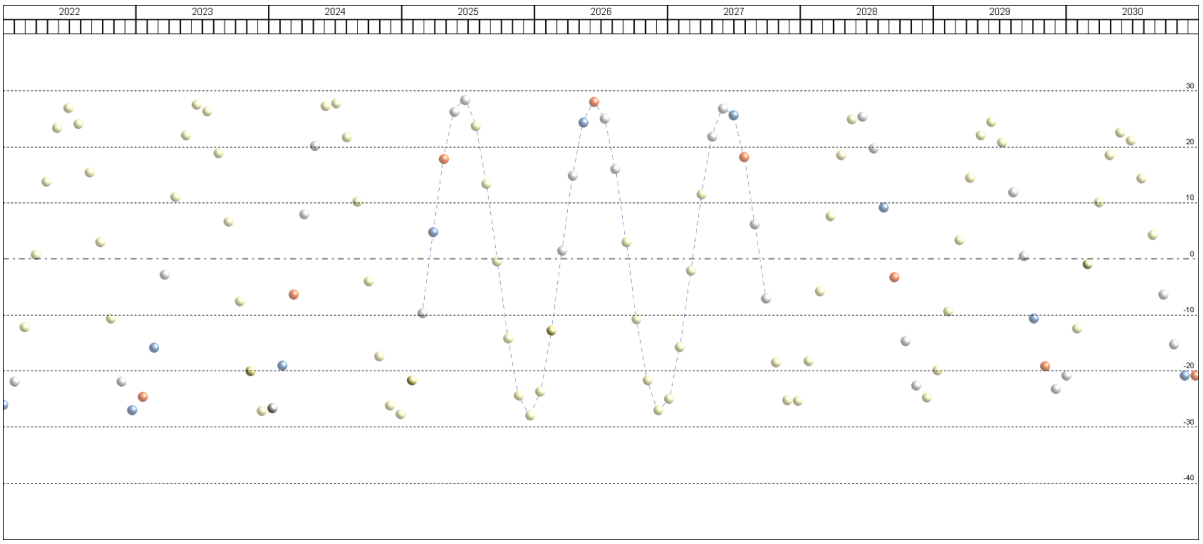

Fig. 13 Between 2022 and 2030, the occurrences of New Moons at perigee with positive declinations relative to the equatorial plane (shown in the upper portion of the graph) are restricted to the years 2025–2027.

The analysis presented in Fig. 13 shows, for example, that between 2022 and 2030 only in the years 2025–2027 do certain New Moon configurations between the Earth and the Sun progressively reach maximum declination values together with orbital distances approaching perigee.

3 The perigee distance also exhibits cyclic variations induced by gravitational perturbations arising from the combined interactions with the Earth, the Sun, and the major planets, implying that the lunar orbit cannot be approximated as a fixed ellipse.

2.3.2.1 Analysis of the Period 1905–30 June 2025 (Part I)

The gravitational interaction exerted by the luni-solar system on a specific point of the Earth's surface is further amplified when the syzygial culmination occurs on the local meridian (in this case, with reference to the longitude of Pozzuoli), that is, when the Moon, during the Earth–Moon–Sun alignment, culminates over central Europe.

The lunar transit across the local meridian is determined by the combined effects of Earth's rotation and the Moon's revolution, while the apparent altitude of the Moon above the local horizon depends on several astronomical factors: the orbital inclination with respect to the ecliptic plane; the geographic latitude of the observer; the Moon's position along its orbit; and the season, which modifies the apparent inclination of the ecliptic.

During transit across the local meridian, the Moon reaches its maximum altitude above the horizon. This altitude increases and decreases symmetrically during its diurnal motion, leading to a reduction in zenith distance and, consequently, to the maximization of the vertical component of the gravitational force exerted on the observation point.

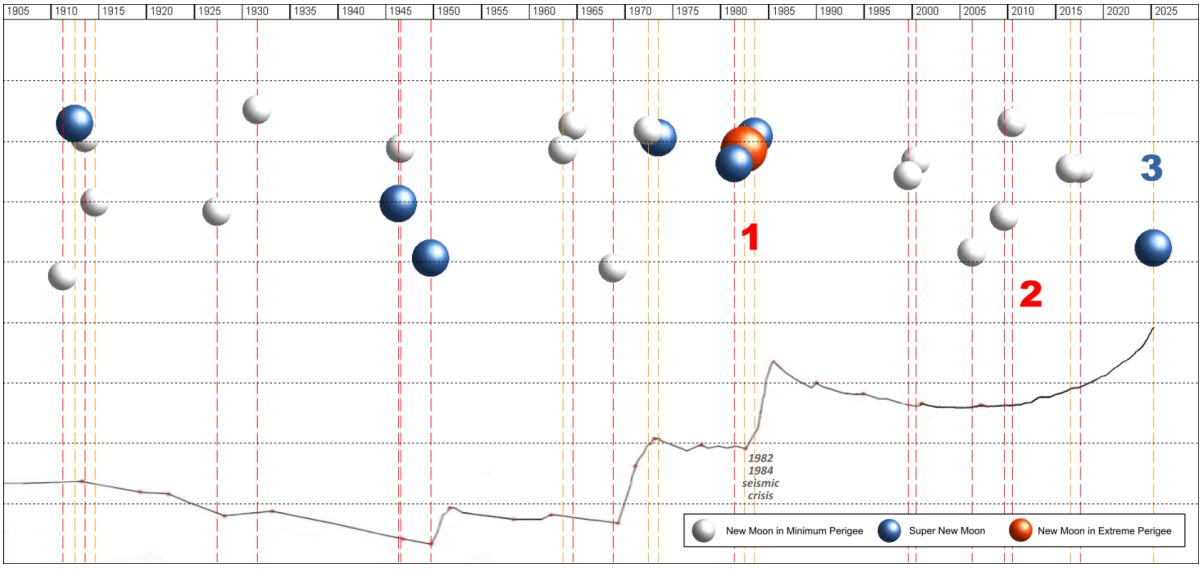

Fig. 14 Period 1905–2025. Ground deformation (bottom) and the 25 Major New Moons (top). At points 1 and 2, the MNMs disrupt the regular correspondence between periodic geometric culminations and the quasi-periodic descending and ascending bradyseismic phases (see points 1 and 2 in Fig. 2, and Figs. 3 and 4).

Fig. 14 illustrates the cases of New Moon, hereafter referred to as Major New Moons (MNMs), corresponding to configurations characterized by: a local altitude ≥ 49°, a perigean distance, and a syzygial culmination aligned with the meridians of Central Europe, between longitudes 1°E and 25°E. According to these selection criteria, among the moons of the 2022–2030 period shown in Fig. 13, only the New Moon of 29 March 2025 can be represented (Point 3).

Considering the New Moons that are simultaneously higher in altitude, closer to the Earth, and orbiting over Central Europe during syzygial culmination, the discrepancies observed in Figs. 2–4 can be coherently explained.

The distribution of the 25 MNMs, filtered according to gravitational and geometric criteria, can be correlated with bradyseismic phases not only in terms of temporal coincidence, but also with respect to the degree of correspondence between the relevance of the astronomical configurations and the magnitude of the associated geophysical phenomena:

- 1982–1984 – The severe bradyseismic phase was preceded and accompanied by three MNMs at Super and Extreme Perigee. The syzygial culminations occurred over Europe at orbital altitudes among the highest of the 1905–2025 period;
- Current phase (2009–2021) – Slower but longer-lasting, it developed in conjunction with seven MNMs over Central Europe, occurring only at Minimum Perigee, with overall lower local altitudes (Fig. 14);

- Previous minor uplift phases (1907–1913, 1928–1933, 1950–1952, 1968–1972) – Correlated with New Moons at Perigee in more isolated configurations;
- 1985–1990 anomaly – Characterized by subsidence instead of the expected uplift, which coincided with the absence of MNMs;
- Frequency of seismic swarms – Higher during the 1982–1984 crisis, while almost absent or significantly reduced during the uplift phases of 1907–1913, 1928–1933, 1950–1952, and 1968–1972.

The configurations represented in Fig. 14 do not occur as discrete events but rather constitute the culmination of a gradual process. Consequently, the gravitational effects are not confined to the exact instant of maximum but are also intensified during adjacent periods—both preceding and following—when the parameters remain close to their extreme values.
In these adjacent intervals, spanning days or even months before and after the peak, similar New Moon configurations and additional daily Moons occurring at Extreme or Super Perigee can be identified. These are represented in Figs. 14–20 by disks colored in red or orange (but not ochre).

2.3.2.2 Analysis of the eruptions of AD 79 and 1538

Relative maximum configurations, characterized by the near-simultaneity of perigee, new moon, and culmination at the local meridian, represent within the cyclic patterns the conditions of maximum lunar gravitational contribution observable at the local scale.
A significant local parameter is the angular distance between syzygy culmination and the meridian of Pozzuoli. This parameter, intrinsically linked to both the geographic configuration of the Campi Flegrei and the Earth's rotation, displays a periodicity close to the diurnal cycle (~24 h) and introduces a perturbation into the more regular and significantly longer lunar cycles previously described. Such perturbation manifests as a disturbing factor in the gradual progression of lunar gravitational oscillations.
Over the course of a year, the Moon is positioned between the Earth and the Sun 12 times—occasionally 13—every 29.5 days during the New Moon phase, amounting to slightly more than 1200 occurrences per century.
From astronomical year 0 to 30 June 2025, a total of 25,044 New Moons have occurred, of which 3,850 were Super New Moons (d < 0.3596 Gm). Among these, during syzygial culmination, 1,395 orbited at Extreme Perigee (i.e., at a distance of less than 357,350 km), 478 of which orbited over the Northern Hemisphere during their culmination.
Of these 478, in the past 2026 years, the New Moons that—at the moment of syzygial culmination with respect to the Earth's axis—orbited in the Northern Hemisphere at Extreme Perigee within the Italo-centric meridians of longitude 5°E to 16°E (corresponding to TT 11:40 to TT 10:56, and the meridians crossing the Gargano region and the areas between Lyon and Marseille) totaled 14:

19-05- 79	11:39:43	0.357321
20-06-0133	11:13:27	0.357345
25-08-0789	11:35:16	0.357124
10-03-0989	11:32:31	0.356926
12-04-1043	11:10:34	0.357239
16-08-1072	11:12:51	0.357012
15-07-1151	11:26:13	0.357252
10-03-1396	11:24:14	0.356920
12-04-1450	10:57:21	0.357093
17-08-1479	11:39:42	0.357132
30-03-1538	11:01:05	0.357061
21-08-1541	11:24:31	0.357226
22-06-1637	10:56:09	0.357317
14-04-1733	11:19:48	0.357207 (Tab. 1)

The VEI alone is not sufficient to assess the geodynamic significance of an eruption, as it is based on surface parameters that do not account for the deeper dynamics of the volcanic system. It is therefore possible that the energy of processes occurring at depth in the years preceding the 1538 eruption exceeded that underlying the major eruptions of Etna or Vesuvio, which followed periods of quiescence shorter than a millennium.
Based on these considerations, the 1538 eruption (VEI 3, according to the Smithsonian Institution) can be classified among the two most significant eruptions in Italy over the past two millennia, being

more relevant than the sub-Plinian eruptions of Vesuvio in 1631 (VEI 4) and Etna in 1669 (VEI 4), despite their higher VEI values.
The eruptions of Vesuvius in AD 79 and Monte Nuovo (in the Campi Flegrei) in 1538 — two of the most significant volcanic events in Italy since year 0 — were both preceded, by about five and six months respectively, by extreme Italo-centric LNM configurations. In the past 2,026 years, only 14 such configurations have occurred. The activity of the Somma–Vesuvius complex is considered together with that of the Campi Flegrei for a couple of reasons. First, research [1] suggests the presence of a single long-lasting magma reservoir extending beneath the entire Naples area. Second, because of their close geographical and structural connection, the luni-solar forces affecting the Campi Flegrei may influence each volcanic system independently — or both at the same time[4].

2.3.2.3 Representation of Lunar Periods and Analysis

The graphical representations (described in the following two paragraphs) include exclusively New Moons with a local altitude ≥ 63°, regardless of geocentric distance, and those with a local altitude ≥ 40° that occurred at Perigee. Daily Culminations are shown without selective constraints. Both categories of New Moons are distinguished according to Earth–Moon geocentric distance, following the classifications reported in Figs. 11 and 12. The New Moons are represented based on local altitude rather than geocentric declination, consistent with the criterion adopted for Culminations.
Each New Moon is marked by a vertical dashed line: in red when the geocentric–equatorial syzygy culminated between meridians 5°E and 25°E, and in orange when it occurred between 1°E and 25°E.

2.3.2.3.1 Analysis of the Period AD 53-79

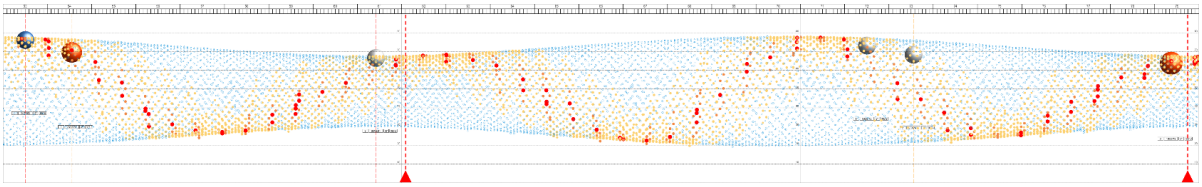

Fig. 15 Period AD 53–79. Lunar Culminations as a Function of Earth–Moon Distance, Central European New Moons.

In Fig. 15, the two red triangles mark the earthquake at Pozzuoli on 5 February AD 62 and the Plinian eruption of Vesuvio on 24 October AD 79, both preceded by a MNM. Between AD 53 and 79, the years 70–71 saw a coincidence between the maximum amplitudes of the first harmonic of the lunar Culmination cycle and the maxima of the second harmonic of Culminations at Perigee. In 61–63 and 79–81, the synchronization of the two cycles entailed in Minimal, Super, and Extreme Perigees at the Culminations of the intermediate years.

2.3.2.3.2 Analysis of the Period 1518-1562

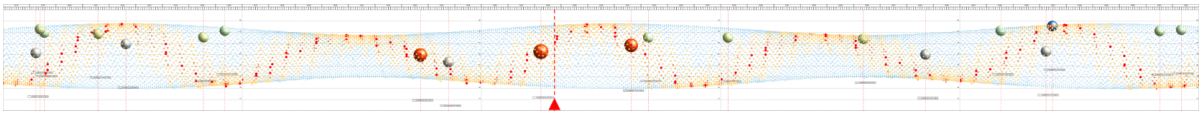

Fig. 16 Period 1518–1562. Lunar Culminations as a Function of Earth–Moon Distance, Central European New Moons.

In Fig. 16, the red triangle indicates the 1538 eruption of Monte Nuovo, preceded by two New Moons at Extreme Perigee. Between 1518 and 1562, three intervals (1521–1522, 1539–1541, and 1557–1558) show a synchronization between the maximum amplitudes of the first harmonic of the lunar Culmination cycle (mean period ~18.6 years) and the maximum amplitudes of the second harmonic of the Culminations at Perigee (mean period ~9 years). In 1531 and 1549, corresponding to the contraction phase of the major harmonic, the synchronization of the two cycles entailed in Minimal, Super, and Extreme Perigees at the Culminations of the intermediate years.

4 "*Nel 79 dopo Cristo il Vesuvio eruttava ed i Campi Flegrei si sollevavano e tremavano*", Professor Antonio Parascandola (1902–1977), "Scienziati studiano il fenomeno del bradisismo. Ore di angoscia a Pozzuoli per la terra che si muove", La Stampa, 1 marzo 1970

2.3.2.3.3 Analysis of the Period 1982–1984

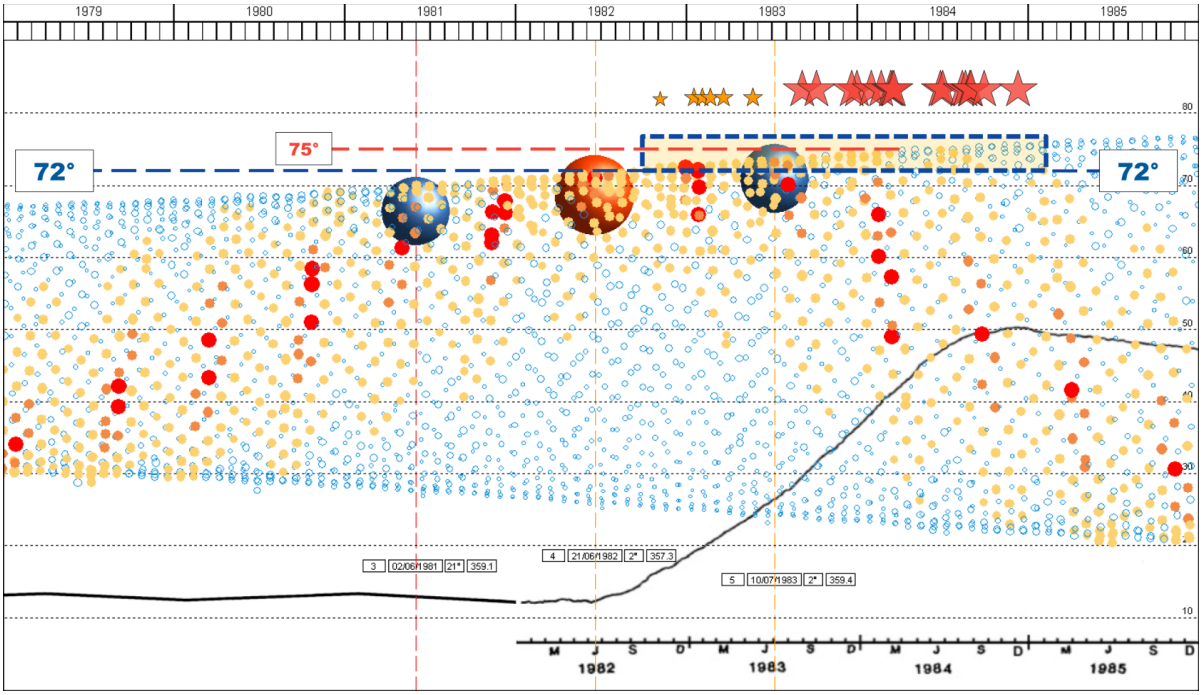

Fig. 17 Period 1979–1985. Culminations according to the Earth–Moon distance, New Moons observed in Central Europe, initial shocks reported by journalistic sources, seismic events with $M_W > 3.6$ (https://terremoti.ov.ingv.it/gossip/) represented by red stars, and ground uplift trends for the years '77–'81 as reported by INGV–OV and for '82–'85 as reported by Aster&Meyer (1988).

According to the record of Aster and Meyer (Fig. 17), the uplift phase at the Campi Flegrei began around mid-June 1982. The onset of ground uplift coincided with the increasing trend in the altitudes of daily Moons and, in particular, with the occurrence of the New Moon at Extreme Perigee on 21 June 1982. The first seismic shocks were detected in November 1982[5], coinciding with the first lunar Culminations at Perigee exceeding 72° in altitude, highlighted by the blue dashed box in Fig. 17. Seismic activity persisted until the last perigean Culminations above this threshold. The seismic swarm of 1 April 1984—comprising about 500 events within an eight-hour interval—and the subsequent slowdown of uplift beginning in mid-May followed a cluster of daily Moons at Minimum, Super, and Extreme Perigee (ochre, orange, and red disks in Fig. 17), associated with decreasing altitudes.

5 "*The first sudden sign of reawakening occurred on November 2: nine shocks of second to third degree, with the epicenter inland north of the center of Pozzuoli, between the Solfatara and Quarto.* (…) *And on January 17, fear returned with a decidedly stronger earthquake, of fourth degree, with the epicenter in the Solfatara.* (…) *Even worse was the evening of February 4: a vigorous jolt, preceded by a dull rumble.* (…) *In April the activity intensified further.* (…) *April 6, second degree. On April 7, at 1:41 and 3:08 a.m., third degree shocks.*" (From *La terra trema da 5 mesi*, *Il Mattino*, April 24, 1983). On April 23, a fourth-degree jolt was felt; on May 19, at 22:15, a seismic swarm lasting two hours was recorded.

2.3.2.3.4 Analysis of the Period 2022–2025

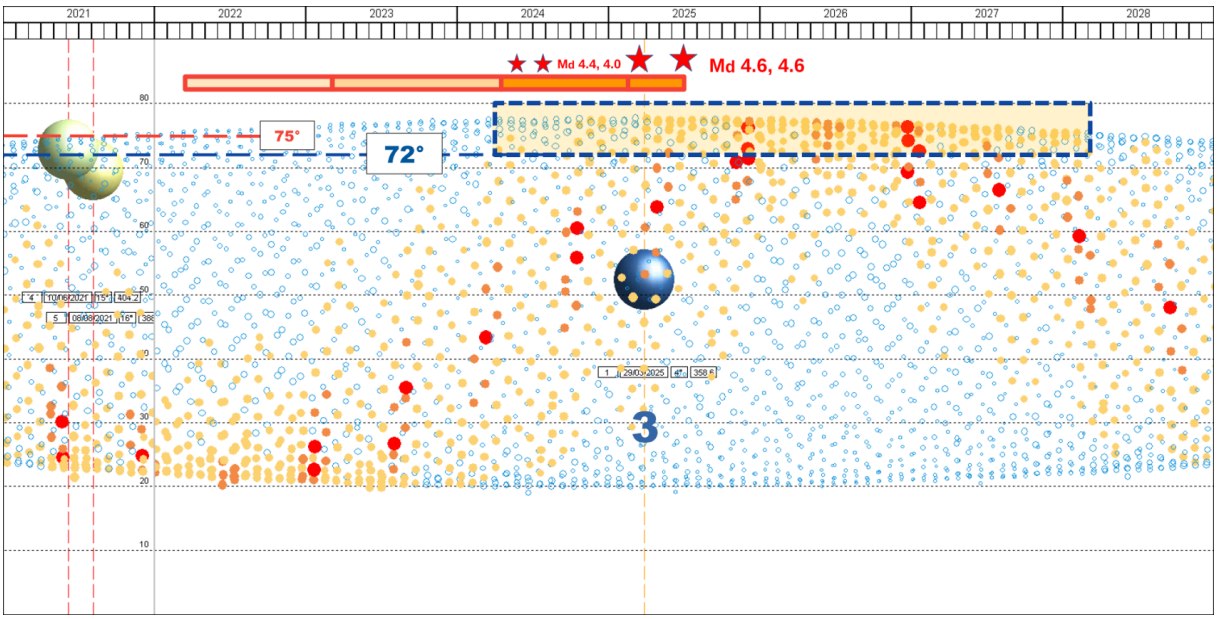

Fig. 18 Period 2021–2027. Culminations as a Function of Lunar Distance and New Moons.
The tripartite band at the top illustrates the evolution, in terms of earthquake frequency, of the ongoing seismic crisis, whose most pronounced initial phase began in March 2022.

Since 29 September 2021, Pozzuoli has been experiencing a period (expected to end on 4 March 2028) of lunar culminations with altitudes exceeding 75° (Fig. 18). The Md 4.4 and Md 4.0 shocks of 20 May and 26 July 2024 were preceded by the first 2–3 minimum-perigee culminations with altitudes greater than 72°, a sequence that will also conclude in early March 2028 (Fig. 18).

2.3.2.3.5 Analysis of the Period 1527–1544

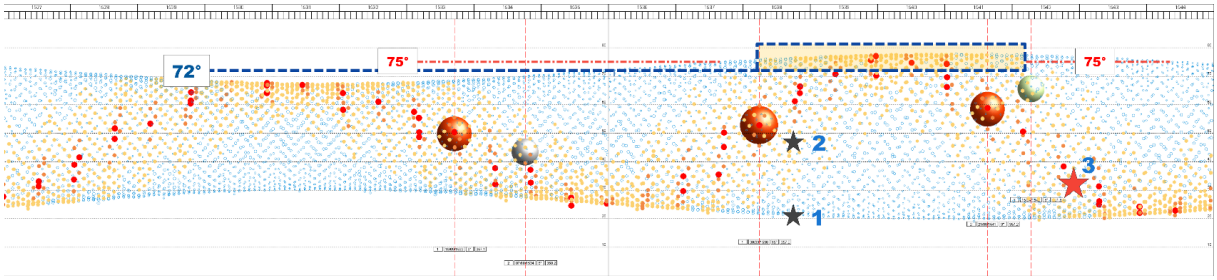

Fig. 19 Period 1527–1544. Lunar Culminations as a Function of Earth–Moon Distance, Central European New Moons, occurrences of the Monte Nuovo eruption of 29 September (star 1) and the explosion of 6 October 1538 that caused 24 casualties (star 2). Star 3 marks the occurrence of the Mw 6.7 earthquake that struck southeastern Sicily in 1542.

Around 20 April 1538, "*frequent earthquakes caused some damage in Pozzuoli and Naples; an increase in activity at the Solfatara was observed*" [2], coinciding with the onset of multiple Moons at least at Minimum Perigee with a local altitude ≥ 72°. "*From June to September 1538, continuous seismicity occurred. Progressive intensification of shocks, not only in Pozzuoli but also in Naples: between five and ten strong tremors per day were reported*" [2]. The Monte Nuovo eruption of 29 September 1538 occurred during the same phase, highlighted by the blue dashed box.

2.3.2.3.6 Analysis of the Period 1905–30 June 2025 (Part II)

(In the plots of bradyseismic trends, the height of the reference ordinate axis was adjusted individually to highlight more clearly the correlation between ground uplift/subsidence phases and lunar orbital dynamics. For the same purpose, the vertical scale of ground deformation was selectively expanded or compressed across the different plots.)
A red diagonally dashed box visually highlights the time interval during which the lunar Culminations exceeded the critical threshold of 75°.

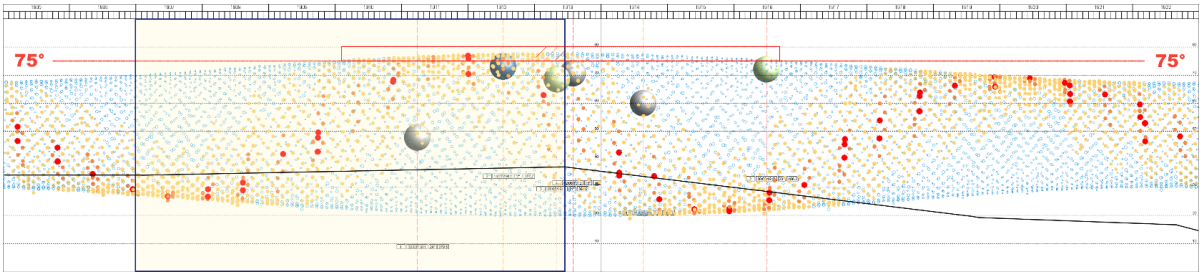

Fig. 20A Period 1905–1922: Ground deformation, lunar Culminations, central european New Moons of the period 1905–1922, with the 1907–1913 uplift and periods with culminations ≥ 75° highlighted by frames.

Given that surveys were conducted at multi-year intervals (IGM 1905, 1913, 1919), it cannot be ruled out that the ascending phase began around 1910, during a year of Culminations with altitudes ≥ 75°, and that the descending phase started around 1916, when Culminations fell below 75°.

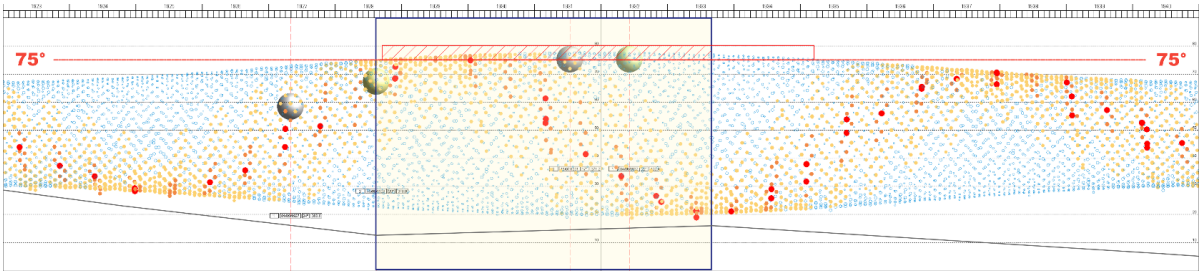

Fig. 20B Period 1923–1940: Ground deformation, lunar Culminations, central european New Moons of the period 1923–1940, with the 1928-1933 uplift and periods with culminations ≥ 75° highlighted by frames.

According to IGM surveys from 1922, (?) 1928, Maio (1933), and Ranieri (1945), the ascending phase began when lunar culminations reached ≥ 75°. The descending phase may have started when culminations dropped below 75°, since no measurements were carried out around the early months of 1935.

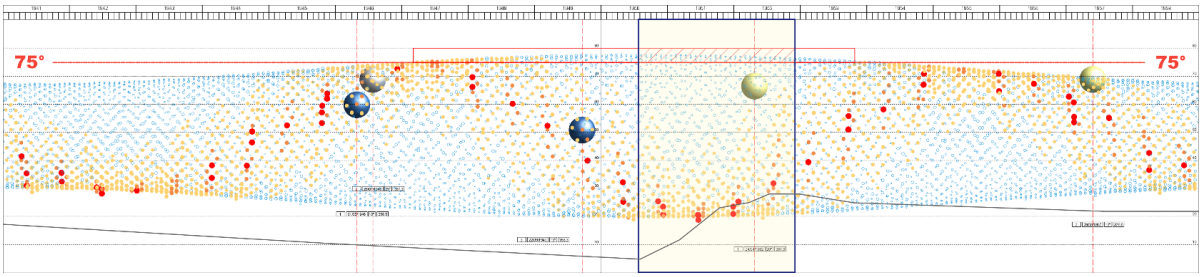

Fig. 20C Period 1941–1958: Ground deformation, lunar Culminations, central european New Moons of the period 1941–1958, with the 1950–1952 uplift and periods with culminations ≥ 75° highlighted by frames.

The ground uplift phase occurred during a period of lunar culminations exceeding 75°, whereas the subsequent subsidence phase coincided with a period when lunar culminations fell below that threshold.

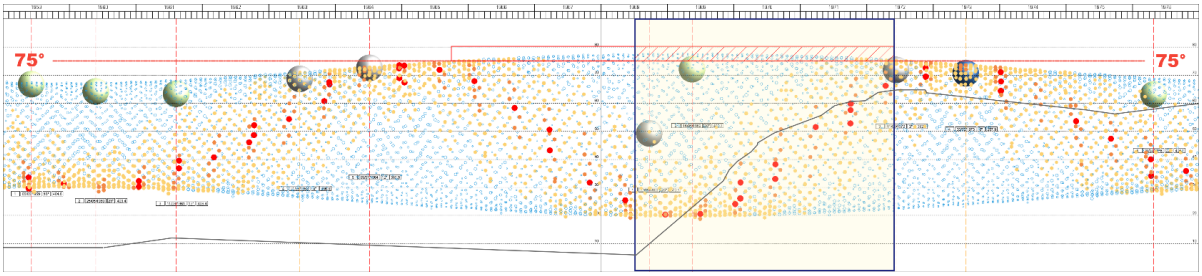

Fig. 20D Period 1959–1976: Ground deformation, lunar Culminations, central european New Moons of the period 1959–1976, with the 1968–1972 uplift and periods with culminations ≥ 75° highlighted by frames.

Similarly, during the bradyseismic crisis of 1968–1972, the uplift phase was confined to the interval with lunar culminations exceeding 75°, whereas the terminal phase—marked by a reduction and eventual cessation of uplift—occurred concurrently with the decrease of maximum lunar altitudes below that threshold.

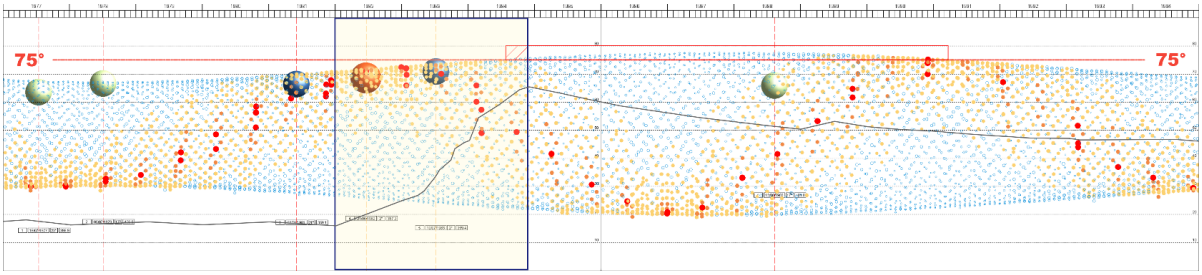

Fig. 20E Period 1977–1994: Ground deformation, lunar Culminations, central european New Moons of the period 1977–1994, with the 1982–1984 uplift and periods with culminations ≥ 75° highlighted by frames.

The first shocks were recorded in November 1982, coinciding with the first lunar culminations at perigee with an altitude exceeding 72° (see Fig. 17).

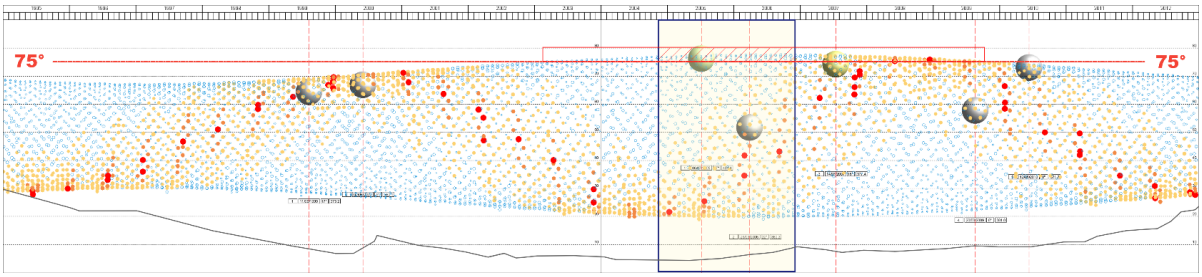

Fig. 20F Period 1995–2012: Ground deformation, lunar Culminations, central european New Moons of the period 1995–2012, with the 2005–2006 uplift and periods with culminations ≥ 75° highlighted by frames.

The reversal of the deflationary trend observed in the biennium 2005–2006 occurred concurrently with a period characterized by lunar culminations exceeding 75° in altitude above the local horizon (Fig. 20F). A previous episode of ground uplift, recorded during the year 2000, took place in coincidence with an increasing trend in the apparent altitudes of Perigee Moons, and with the occurrence of two New Moons classified as Elevated and Central European at Minimum Perigee.
The rapid increase in uplift rate recorded in 2012, for which a magmatic intrusion hypothesis has been proposed [3], coincided temporally with the New Moon of 20 May 2012. However, this lunar event was not included in the comparative analysis, as it does not fall within the category of Central European New Moons according to the criteria adopted in this study (Fig. 20F).

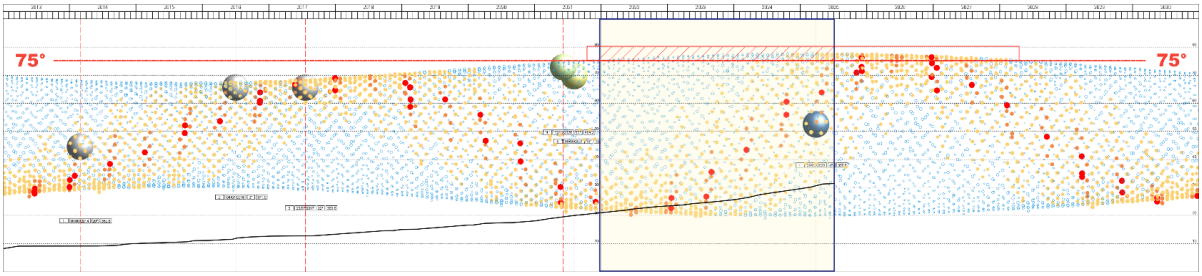

Fig. 20G Period 2013–2030: Ground deformation, lunar Culminations, central european New Moons of the period 2013–2030, with the 2022–2025 uplift and periods with culminations ≥ 75° highlighted by frames.

The most pronounced phase of seismic activity in the Campi Flegrei caldera began around March 2022. Since 29 September 2021, Pozzuoli has been experiencing a period (expected to end on 4 March 2028) of lunar culminations with altitudes exceeding 75°.

2.3.2.3.7 Harmonic synchronization during the period 1419–2138

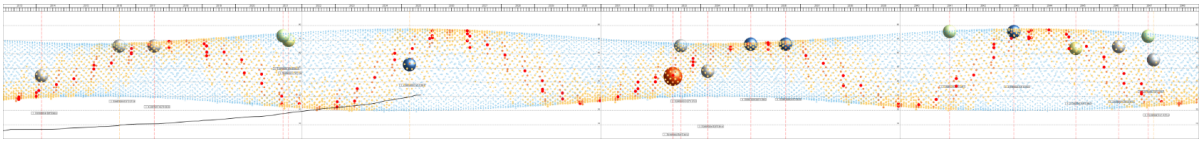

Fig. 21 Period 2013–2048: Bradyseismic trend 2013–2025, daily culminations according to Earth–Moon distance, and the MNMs of the period 2013–2048.

Between 2013 and 2048, on two occasions (2025 and 2043–2044), the maximum amplitudes of the first harmonic associated with the lunar culmination cycle (average period ~18.6 years) coincided with the maxima of the second harmonic of perigee culminations (average period ~9 years). During 2016–2017 and 2034–2036, at the narrowing of the harmonic, synchronization between the two cycles corresponded to perigee distances classified as Minimum, Super, and Extreme, occurring at lunar culminations with elevated altitudes (though below the absolute maxima) within the intermediate interval between the two peaks. Over the period 1419–2138, the closest synchronizations occurred at intervals of ~150–200 years, specifically in 1522/1541, 1671/1690, 1876/1894, and 2043/2062 (Fig. 22).
The two harmonic components exhibit a periodicity ratio close to 2:1, leading to periodic synchronization of both maxima and minima. Synchronized minima may exert a compensatory effect, partially offsetting the lack of maxima, with an overall influence that could remain relatively constant over time, thereby attenuating temporal variability in the lunar gravitational attraction.
The synchronizations of 1671 and 1690 temporally preceded a sequence of major seismic events (Mw 6.6–7.3) that occurred between 1688 and 1706, including the earthquakes of 1688, 1693, 1694, 1702, two in 1703, and one in 1706, with magnitudes of Mw 7.1, 7.3, 6.7, 6.6, 6.9, 6.7, and 6.8, respectively.
The synchronizations identified in 1876 and 1894 preceded a high-energy seismic sequence between 1905 and 1920, characterized by main events with moment magnitudes ranging from Mw 6.5 to 7.1, occurring in 1905, 1908, 1915, and 1920 (Mw 7.0, 7.1, 7.1, and 6.5, respectively). This phase also included the peculiar seismic crisis of the Tuscan–Emilian Apennines in 1916–1920, which comprised six events with Mw values of 5.8, 5.8, 6.0, 6.0, 6.4, and 6.5. [13]

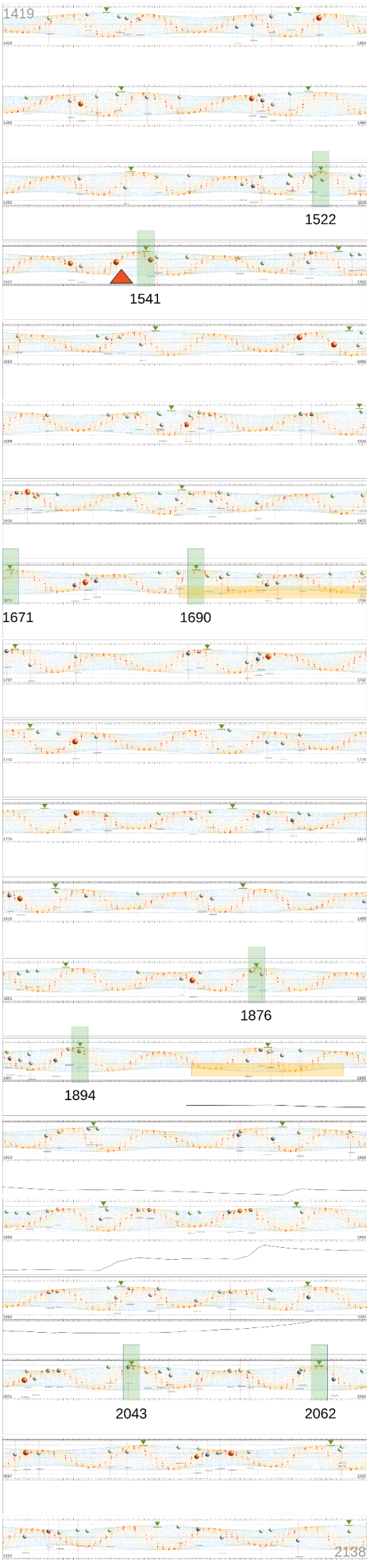

Fig. 22 Period 1419–2138. The time series of daily culminations by Earth–Moon distance, the MNM, the occurrence of the Monte Nuovo eruption of 1538, and the maximum synchronizations—boxed and shaded in green—between the harmonic associated with the cycle of lunar culminations and the harmonic of perigee culminations, seismic storms boxed and shaded in orange

2.3.2.3.8 Rates of ground uplift (1961–2025)

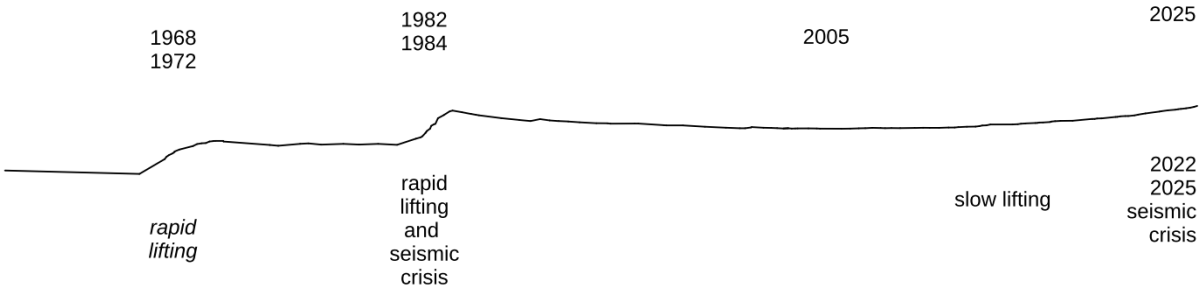

Fig. 23 Period 1961–2025. The trend of vertical ground deformation is shown with an amplified vertical scale in order to highlight more clearly the relative differences between the uplift episodes of 1968–1972, 1982–1984, and the current phase, which is characterized by significantly lower deformation rates.

The bradyseismic crises of 1968–1972, 1982–1984, and 2022–2025 have been characterized by significant differences in both seismic response and ground deformation. During the 1968–1972 phase, the total uplift (~170–180 cm) was comparable to that observed in 1982–1984, but seismicity was almost entirely instrumental in nature and rarely perceived by the population. In contrast, the 1982–1984 crisis was accompanied by over 10 000 earthquakes, with very high daily occurrence rates and numerous felt events. The 2022–2025 phase is showing an intermediate behavior: seismic swarms are less numerous than in the 1980s, but include isolated events of higher magnitude (up to Mw 4.6). Uplift is slower (1–3 cm/month) but cumulatively substantial (> 1.4 m since 2005).
The vertical ground deformation record, displayed with an amplified vertical scale to more clearly highlight relative differences among uplift episodes, does not reveal any correlation between uplift rates and the seismic energy released during the respective bradyseismic crises of 1968–1972, 1982–1984, and 2022–2025.

2.3.3 Observational Correlations and limitations of the current paradigm

Italy is characterized by a widespread presence of active, quiescent, and fossil volcanism affecting large portions of the national territory. In addition to the well-known active volcanic complexes in southern areas, the occurrence of inactive or extinct volcanic edifices in the northern regions (such as Monte Amiata, the island of Capraia, the Euganean Hills, and the Valsesia supervolcano) provides evidence of a significant magmatic evolution relevant to the understanding of regional geothermal processes. Thermal evidence indicates the presence of active magmatic bodies at varying depths. These bodies contribute to intrusion phenomena and the ascent of hot fluids, with surface manifestations such as thermal springs and fumarolic activity. Such features attest to a widespread volcanic framework that is not confined exclusively to the most prominent volcanic structures. Recent studies [4] indicate that deep magmatic intrusions can generate distinctive seismic signals and actively contribute to the evolution of the crustal stress state. Consequently, the genesis of some high-magnitude earthquakes may not be exclusively tectonic in origin but may be influenced—or in certain cases even triggered—by magmatic processes.
Seismicity in the Italian territory is traditionally interpreted in tectonic terms, in relation to the complex convergent dynamics between the African and Eurasian plates. However, a growing body of geophysical, geochemical, and structural evidence suggests that several areas of the peninsula (including sectors of the northern Apennines, the Tyrrhenian margin, and parts of the Alpine arc) are affected by latent volcanism. This perspective requires a critical reassessment that explicitly considers the interaction between active tectonic systems and deep magmatic dynamics, even in regions previously regarded as having low or negligible volcanic potential.
Such processes may influence seismicity through the interaction of magmatic intrusions with active faults. Strictly speaking, it would be methodologically correct not to mention the observational correlations presented below; however, their systematic omission risks overlooking potentially relevant data. Although the absence of a verified causal link between lunar–solar configurations and seismic activity requires caution in interpretation, the systematic exclusion of such correlations may conceal weak yet potentially significant signals relevant to Earth system dynamics. From a methodological standpoint, avoiding the inclusion of such observations may be justified in

accordance with the criteria of scientific verifiability and falsifiability. Nevertheless, excluding them entirely could also imply disregarding alternative hypotheses which, though currently speculative or unconfirmed, may gain relevance in light of future theoretical or technological advances.
The exclusion of such observations could lead to the conclusion that certain lunisolar configurations did not exert significant effects on the Earth's lithosphere. In this context, it should be noted that the relationship between lunar cyclicity and seismic activity has been discussed in the literature [5][6].

2.3.4 Other Correlations between solstitial lunar–solar configurations and significant geophysical events

Over the entire period 0–2100, 27 New Moons occurred between 14 and 28 June (21 June ±7 days, near the summer solstice, when the inclination of Earth's axis allows for the highest luni-solar altitudes in the Northern Hemisphere), between longitudes 0° and +27°, during the culmination of the syzygy phase relative to the Earth's axis, with declinations greater than 0° on the equatorial plane, and orbiting at distances shorter than 0.377 gigameters from Earth.
Excluding 17 remote or future dates, of the remaining 10, three or four fall in temporal correspondence with significant events in the Vesuvio–Campi Flegrei volcanic arc:

- 26 June 1302 preceded by 32 days the last eruption at Ischia (Campi Flegrei). This was an important event in the island's geological history and represents the last documented eruption;
- It cannot currently be ascertained with certainty whether the lunar configuration of 26 June 1557 preceded or followed the earthquake of the same year that caused the collapse of the church in the village of Campagnano (Ischia), owing to the lack of precise dating for the latter.
- In mid/late June 1982, according to a graph by Aster and Meyer (1988), the ascending bradyseism at Campi Flegrei began, ending in the very early days of 1985;
- 25 June 2025 preceded by 5 days the 30 June earthquake of magnitude Md 4.6, the strongest event at Campi Flegrei at least since 1584 (together with that of 13 March 2025);
- The 16 configurations dated between 114 and 1240, marked with the symbol (◦), may not have produced surface manifestations because the onset of events is conditioned by the dynamic state of the Campi Flegrei–Vesuvio volcanic system, which had already been structurally modified by the Plinian eruption of AD 79.

01.	(◦)	20-06-0114	10:57:01	0.365051
02.	(◦)	20-06-0133	11:13:27	0.357346
03.	(◦)	20-06-0152	10:55:29	0.368138
04.	(◦)	16-06-0459	11:59:39	0.365032
05.	(◦)	25-06-0469	11:51:02	0.357482
06.	(◦)	16-06-0497	11:56:33	0.368131
07.	(◦)	20-06-0540	10:16:50	0.357400
08.	(◦)	25-06-0857	11:30:00	0.370280
09.	(◦)	16-06-0866	10:46:28	0.365402
10.	(◦)	25-06-0876	11:01:02	0.357714
11.	(◦)	16-06-0885	11:05:26	0.357394
12.	(◦)	26-06-0895	11:37:08	0.363302
13.	(◦)	16-06-0904	10:59:35	0.367765
14.	(◦)	26-06-1150	11:47:46	0.359013
15.	(◦)	21-06-1221	11:25:39	0.357706
16.	(◦)	21-06-1240	11:51:15	0.363230
17.		26-06-1302	10:13:03	0.363009
18.		26-06-1557	11:25:31	0.359434
19.		22-06-1618	10:48:38	0.366031
20.		22-06-1637	10:56:08	0.357318
21.		22-06-1656	10:58:55	0.367038
22.		18-06-1708	10:19:09	0.357816
23.		21-06-1963	11:45:56	0.366355
24.		21-06-1982	11:52:57	0.357328
25.		21-06-2001	11:59:27	0.366700
26.		25-06-2025	10:17:06	0.366753
27.		16-06-2053	10:37:12	0.357745

(Tab. 2)

Based on the considerations of the previous paragraph, with the exception of the 1982 date, the 7 configurations between 1618 and 2001 listed in Tab. 2 are not directly associated with seismic events at the Campi Flegrei. However:

- Less than one month after the conjunction of 21 June 2001, at Etna, between 13 and 17 July, 28

shocks of magnitude 3.5–4.0 occurred in the area;
- Less than one month after the configuration of 21 June 1963, on 9 July 1963, a magnitude 6 earthquake struck the Ligurian Sea;
- Seven months after the lunisolar configuration, on 29 January 1657, a magnitude 6 event hit the Capitanata area;
- A magnitude 6.8 earthquake occurred on 8 June 1638 in the Crotone region, though one year after the lunisolar date of 1637;

No significant shock followed the configuration of 18 June 1708. Between 1688 and 1706, Italy was struck by a series of strong earthquakes with magnitudes ranging from 6.6 to 7.3. The sequence of seismic events may have released much of the stress accumulated along active faults, potentially reducing the residual seismogenic potential in the area, at least in the medium term.

Similarly, based on the considerations of the previous paragraph, most of the configurations in Tab. 1 are not associated with geophysical events in the Campi Flegrei–Vesuvio volcanic arc. However:

- On 25 October 989, a magnitude 6.9 earthquake occurred in Irpinia (Campania), seven months after the configuration of 10 March 989;
- After 22 June 1637, but nine months later, on 27 March 1638, a Mw 7.1 earthquake struck Calabria;
- Following the date of 12 April 1450, but about seven years later, on 5 December 1456, a Mw 7.2 earthquake hit the Irpinia area (Campania). Concerning the 1456 earthquake—"*uno dei maggiori che abbia scosso l'Italia meridionale, abbiamo anzitutto ad osservare la solita discrepanza delle date: alcuni lo fanno accadere nel 1448, altri nel 1449 o nel 1450 od anche nel 1457"* [8].

19-05- 79	11:39:43	0.357321
20-06-0133	11:13:27	0.357345
25-08-0789	11:35:16	0.357124
10-03-0989	11:32:31	0.356926
12-04-1043	11:10:34	0.357239
16-08-1072	11:12:51	0.357012
15-07-1151	11:26:13	0.357252
10-03-1396	11:24:14	0.356920
12-04-1450	10:57:21	0.357093
17-08-1479	11:39:42	0.357132
30-03-1538	11:01:05	0.357061
21-08-1541	11:24:31	0.357226
22-06-1637	10:56:09	0.357317
14-04-1733	11:19:48	0.357207 (Tab. 1)

The New Moon of 30 March 1538, which occurred at extreme perigee and was preceded by a comparable configuration (Fig. 19), represents a distinctive dynamical case.
To investigate analogous configurations, an analysis was performed to identify New Moon phases similar to that of 30 March 1538 (Fig. 19; Tab. 1), which occurred approximately six months before the Monte Nuovo eruption. The selection criteria took into account orbital conditions consistent with those of 1538, specifically a comparable Earth–Moon–Sun geometry, characterized by the Earth being at the same seasonal orbital position and with an equivalent axial tilt relative to the Sun.
Within the chronological interval 0–2100 AD, three New Moon events were identified between 29 and 31 March (i.e., within ±1 day of 30 March), occurring at syzygy culmination between geographic longitudes +2° and +19°, with positive lunar declination relative to the equatorial plane and a geocentric distance of < 0.3596 Gm.

01.	29-03-0990	10:54:24	0.358997
02.	30-03-1538	11:01:04	0.357062
03.	29-03-2025	11:48:00	0.358642 (Tab. 3)

The magnitude 4.6 earthquake recorded on March 13, 2025, in the Campi Flegrei area, one of the two strongest in the region, along with the one on 30 June 2025, at least since 1584, occurred in close temporal proximity to the New Moon phase of 29 March 2025 (but anticipating it[6]).

6 The earlier occurrence of the seismic event may be linked to a secondary parameter, identified but not yet fully investigated or included in the current analysis.

In the period 2010–2027, eight New Moons occurred, orbiting at the height of the syzygial phase on the meridians between longitudes 2°E and 33°E and with declination greater than 0 and a distance from Earth less than 0.37350 gigameters:

01.	12-06-2010	11:29:16	0.371746	73°
02.	20-03-2015	10:18:43	0.357947	47°
03.	07-04-2016	09:51:20	0.357266	49°
04.	04-07-2016	11:49:51	0.371991	65°
05.	23-07-2017	10:35:02	0.363631	65°
06.	29-03-2025	11:47:59	0.358641	52°
07.	25-06-2025	10:17:05	0.366753	73°
08.	02-08-2027	10:02:42	0.357383	62°

(Tab. 4)

The two strongest tremors at Campi Flegrei since at least 1584 were recorded on 30 June 2025, and March 13, 2025. Two of the eight dates precede the three earthquakes of magnitudes 6.0, 5.9, and 6.5 that struck Central Italy in 2016, from August to the end of October.

The analysis of bradyseismic data reveals an episode of rapid uplift in 2012 (Fig. 24, upper-right section), interpreted as a possible effect of magmatic intrusion [3]. This abrupt increase in uplift rate may have been modulated by the New Moon phase of 20 May 2012, not shown in the graphs as it was not visible at its syzygial culmination within the Central European domain. Based on the data available at the end of 1975 and 1976, and in the absence of intermediate measurements between April and May 1976, it can be hypothesized that the pronounced bradyseismic uplift recorded between 1975 and 1977 may have begun in the last days of April 1976 (Fig. 24). The New Moons of 29 April 1976 and 21 May 2012, both belonging to Saros cycle No. 128 and separated by exactly 6585 × 2 days (≈36 years), were not included in the comparative analysis, as they do not fall within the category of Major Central European New Moons (MNM) according to the criteria adopted in this study. It is nevertheless noteworthy that, coinciding with uplift episodes, both preceded by eight days two seismic events of exceptional significance for the Italian context: the Friuli earthquake (Mw 6.5; 6 May 1976; 990 fatalities) and the Finale Emilia earthquake (Mw 5.8; 29 May 2012; 20 fatalities).

The New Moon of 29 April 1976, which occurred as an eclipse with its umbral maximum over Northern Africa and culmination along the meridians crossing the Strait of Otranto, was not included among the 24 MNM in the 1905–2029 dataset, due to its Earth–Moon distance (> 0.373500 Gm), exceeding the minimum perigee threshold. Similarly, the New Moon of 20 May 2012 also occurred as an eclipse, but at a non-perigean orbital distance and was not observable from Central Europe. In this case, an Mw 5.9 earthquake (7 fatalities) struck Finale Emilia approximately 20 hours before syzygy. A further New Moon with analogous orbital characteristics occurred on 21 April 2012.

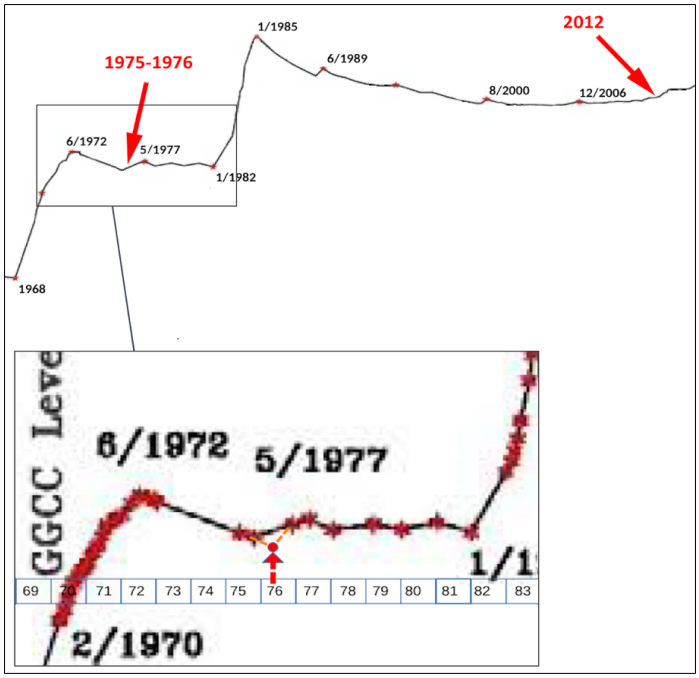

Fig. 24 The bradyseismic trend at Campi Flegrei from 1967–2015 (top) and from 1969–1983 (bottom) [9]

2.4 Temporal Correlations between the most notable reciprocal configurations of the three main external gravitational sources and the main geophysical phenomena

The Moon, the Sun, and Jupiter are the primary external sources of gravitational forces acting on planet Earth, influencing phenomena such as tides (Moon and Sun), satellite orbits, and, to a lesser degree, the orbital dynamics of the Earth–Moon system.
Gravitational influences of Jupiter on Earth do exist, but they are extremely weak compared to the forces exerted by the Sun or the Moon. Over very long timescales (millions of years), however, the combined gravitational effects of the giant planets (particularly Jupiter and Saturn) may contribute to small secular variations in the orbits of planets and satellites.
Attempts to establish a link between planetary dynamics and seismic activity have been addressed in the literature [10].
Here, it is shown how the planet has been configured at extremely narrow angular distances with the Moon and the Sun prior to relevant geophysical events recorded in the Campi Flegrei–Vesuvius volcanic arc.

2.4.1 Correlations between geocentric equatorial configurations and major geophysical events

Among the 25,986 New Moons (Moon+Sun) occurring in the astronomical period 0–2100, those at Extreme Perigee (distance ≤ 0.35735 gigameters) number 1,437.
Close Sun–Jupiter conjunctions, with a minimum mutual angular distance of 0.2°, amount to 212.
The two types of conjunction (New Moon in right ascension at Extreme Perigee, and Sun–Jupiter conjunction in right ascension—i.e., relative to Earth's rotation axis, in a geocentric equatorial reference system) occurred simultaneously on only two occasions: 21–23 December 181 and 22–23 December 1367. Narrowing the lunar distance threshold from 0.35735 to 0.3567 Gm yields only one match: the Moon–Sun–Jupiter conjunction of 21–23 December 181. According to some sources, such as the Italian Wikipedia entry "Supervolcano" (accessed September 9, 2025), the most violent eruption of the last 5,000 years occurred in 181 AD[7].
The closest Moon-Sun-Jupiter conjunction coincided with the year of what was likely the most violent historical eruption of the last 5,000 years.
Extending the lunar distance threshold from 0.3567 to 0.377 Gm, we obtain 19 occurrences:

01.	23-12-0181	20:21:44	0.356685	
02.	22-06-0282	23:36:02	0.367288	
03.	17-06-0353	21:33:56	0.363255	
04.	13-12-0418	14:22:17	0.373921	
05.	12-06-0424	20:51:10	0.360201	
06.	08-12-0489	11:03:52	0.368738	
07.	08-06-0495	19:20:18	0.358321	
08.	26-06-1302	10:13:03	0.363009	
09.	22-12-1367	01:36:56	0.357012	
10.	21-06-1373	08:20:04	0.366723	
11.	16-12-1438	23:52:23	0.358223	
12.	16-06-1444	07:05:12	0.371186	
13.	11-12-1509	21:53:23	0.360815	
14.	12-06-1515	04:24:23	0.376411	
15.	06-12-1580	19:25:19	0.364401	
16.	08-01-1712	09:43:44	0.362704	
17.	04-07-1883	15:50:59	0.376674	
18.	30-06-1954	12:22:39	0.371406	
19.	25-06-2025	10:17:06	0.366753	(Tab. 5)

7 The determination of the year was estimated on the basis of historical chronologies: some Chinese chronicles report "red skies," "dry fogs," and solar anomalies in the years between 180 and 185 AD. In the West as well, there are vague testimonies of a cold or unstable climate. The great eruption dated to 181 AD was initially attributed to the Taupo supervolcano, located in the center of New Zealand's North Island. More recent studies of the Taupo volcano, based on dendrochronology and tephrochronology, have instead dated the VEI 6 Hatepe eruption to 232 ± 5 AD. Nevertheless, there remain indications pointing to a major volcanic eruption in 181, even though it is not known with certainty which volcano was responsible; it might have been a tropical or equatorial eruption for which no direct geological traces have yet been identified.

Four dates of the 19 listed Moon-Sun-Jupiter conjunctions closest in R.A. (minimum angle of 0.2°) occurred prior to significant geophysical events in the Phlegraean-Vesuvian area:

- June 1302 preceded by 32 days the last eruption at Ischia (Campi Flegrei). This was an important event in the geological history of the island and represents its last documented eruption.
- 8 January 1712 preceded by 28 days the first manifestations of the 5 February effusive eruption of Vesuvius, which lasted 126 days. It was one of many eruptions of the 17th and 18th centuries and was not particularly violent.
- 4 July 1883 preceded by 24 days the catastrophic Casamicciola earthquake (Ischia, Campi Flegrei) of 28 July (Mw 4.2, 2,313 fatalities) and by 51 days the great historic Krakatoa eruption (VEI 6, 20 May 1883), whose atmospheric wave reverberations were recorded worldwide.
- 25 June 2025 preceded by 5 days the 30 June earthquake of magnitude Md 4.6, the strongest event at Campi Flegrei at least since 1584 (together with that of 13 March 2025).
- Below 0.407 Gm and with a minimum angular distance of 0.6°, among the 14 pairings identified between 1800 and 2030 (in addition to those already listed), one further case emerges: 1 August 1943, which preceded by 5 months the last eruption of Vesuvius (1944, 21 fatalities).

2.4.2 Correlations between European configurations and major geophysical events

Throughout the entire period 0–2100, only 19 New Moons are found to have occurred at any lunar distance and altitude over the European meridians (between longitudes –11° and +27°, corresponding to TT 12:44 and 10:12), during the culmination of the syzygy phase relative to Earth's axis, and coinciding, within ±2 days, with a close Sun–Jupiter conjunction (maximum angular distance of 1.1°).

01.		27-10-0037	11:52:50	0.366517
02.	(∘)	28-05-0222	11:21:34	0.364220
03.	(∘)	24-07-0271	10:35:02	0.406066
04.	(∘)	13-11-0334	11:38:37	0.398937
05.	(∘)	14-01-0408	11:52:50	0.406201
06.	(∘)	08-12-0489	11:03:52	0.368738
07.	(∘)	29-10-0547	11:45:07	0.406658
08.	(∘)	29-06-0721	11:27:13	0.405155
09.	(∘)	14-05-0945	11:45:16	0.364968
10.	(∘)	04-06-1076	10:54:10	0.399283
11.		21-10-1199	10:57:24	0.372546
12.	(*)	16-10-1270	10:14:31	0.377531
13.		26-06-1302	10:13:03	0.363009
14.		11-05-1526	11:29:39	0.405939
15.	(*)	09-08-1801	12:07:32	0.404130
16.		04-05-1905	12:43:13	0.403010
17.	(^)	30-06-1954	12:22:39	0.371406
18.		29-04-1976	10:34:03	0.405110
19.		25-06-2025	10:17:06	0.366753

(Tab. 6)

In addition to the already described dates of 1302 and 2025, several among these 19 configurations occurred shortly before events of clear relevance in the Campi Flegrei–Vesuvius volcanic arc:

- 11 May 1526 falls within the seismic phase preceding the Monte Nuovo eruption (Campi Flegrei).
- 4 May 1905 preceded both the largest Vesuvius eruption of the 20th century (April 1906) and the onset of the first ascending bradyseism documented between 1907 and 1913, following centuries of continuous subsidence since the Monte Nuovo eruption of 1538 (Fig. 25)[8].
- 29 April 1976 preceded the marked increase in uplift rate that can probably be dated to 1976 (Fig. 25), following the long and pronounced subsidence phase subsequent to the 1968–1972 bradyseismic crisis.
- 25 June 2025 anticipated by 5 days the Md 4.6 shock of 30 June 2025, one of the two strongest earthquakes at Campi Flegrei at least since 1584.
- AD 37 and 1199 may be correlated with two significant paroxysmal episodes in the volcanic area, provided that the events are backdated by approximately one year:

8 The date of 4 May 1905 preceded by four months the major Mw 6.95 earthquake of 8 September in Calabria (558 fatalities), which marked the onset of the seismic storm with magnitudes ranging from Mw 6.5 to Mw 7.1 between 1905 and 1920. This sequence included the 1905, 1908, 1915, and 1920 events, as well as the Tuscan–Emilian Apennine crisis of 1916–1920 (Mw 5.8, 5.8, 6.0, 6.0, 6.4, 6.5).

- the collapse of the lighthouse tower at Capri (seismic crisis dated AD 37–38)[9]
- the phreatic explosion at Solfatara in 1198 (Campi Flegrei) [10]

(◦) The nine configurations between 222 and 1076 may not have produced any surface events. Gravitational geometric configurations are subordinate to the state of the volcanic system, in this case to the restructured state resulting from the Plinian eruption of AD 79.

(*) The dates of 1270 and 1801 were not followed by significant events. It can be noted that during these years the planet Jupiter was orbiting at aphelion (at 5.4 and 5.3 AU, respectively), a condition that also implies maximum relative distance from the Earth. By contrast, all the other dates identified between 1302 and 2025 (with Jupiter at distances of 5.2, 5.04, 4.98, 5.16, 4.97, and 5.14 AU, respectively), while on 21 October 1199 Jupiter was at aphelion, 5.4 AU from the Sun.

(^) The date of 30 June 1954 preceded by just over two months the Mw 6.7 earthquake in Algeria (in the Northern Hemisphere) on 9 September. The New Moon of 30 June manifested as a total solar eclipse, with maximum visibility over the northern seas of the United Kingdom and a syzygy culmination along the meridians crossing Morocco and Algeria. Similar earthquakes in the same area since 1973 occurred only in 2003 (Mw 6.8) and in October 1980 (Mw 7.3).

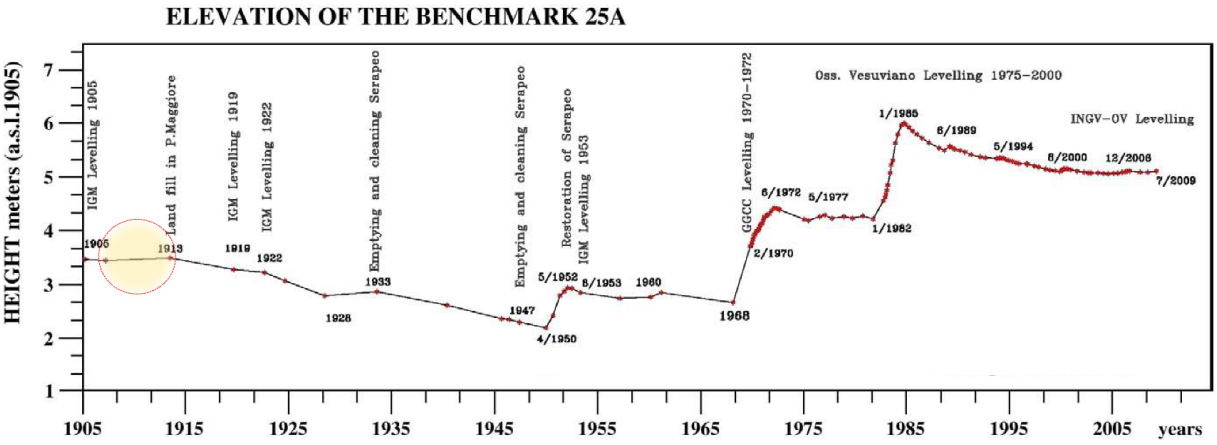

Fig. 25 Ground deformation at Campi Flegrei between 1905 and 2009 (Benchmark 25A). (C. Del Gaudio et al. /Journal of Volcanology and Geothermal Research 195 (2010) 48-56). 6). The ground uplift from 1907 to 1913 highlighted with a circle.

9 The most recent chronological reconstructions by historians, which take into account differences among ancient dating systems, overlaps between civil years and regnal years, as well as ambiguities in the sources, place the seismic and bradyseismic events described between March 37 and early 38 AD. The precise dating of these events is complicated by the fact that the sources are not geological but historical, and often symbolic or propagandistic in nature. Moreover, bradyseismic phenomena may have a progressive duration; thus, an event that began in 37 could have produced evident manifestations well into the early months of 38.

10 The 1198 event, "*reported in the historical tradition of Italian seismological catalogues from Bonito (1691), Mercalli (1883), and Baratta (1901) up to those currently in use (CPTI 1999, 2004)*" [11], was considered by Scandone, D'Amato, and Giacomelli (2010) [12] to be, at most, a minor phreatic explosion. Guidoboni and Ciuccarelli (2011) [11], based on a critical re-evaluation of the sources, concluded that the 1198 eruption did not occur, since the available information derives from contaminated and spurious literary traditions, as well as from the absence of contemporary records for the period in question. The New Moon of 21 October 1199 may be too distant from the more widely accepted 1198 date, although the latter is itself based on retrospective sources, often written two or three centuries after the event. Vecchio et al. (1995) found no evidence of recent eruptive deposits above the ruins of a Roman necropolis near the Solfatara. However, at the same site, they identified retaining walls along the road from Naples to Pozzuoli, dated no earlier than the late 12th century. This dating is compatible with the presumed eruption and the earthquake that caused damage in Pozzuoli, as reported by Mazzella (1591) and Capaccio (1604) [12]. The precise dating remains uncertain, owing both to the limitations of historical sources and to the lack of reliably datable geological evidence. The event is most plausibly placed within a time window spanning from the late 12th to the early 13th century. At present, it seems more likely that the alleged event occurred prior to the triple conjunction of 21 October 1199.

2.5 Method for calculating MNMs

2.5.1 Universal Times and Geographic Longitudes. The meridian sector between Longitudes +1 and +25 and the time interval TT 10:20–11:56.

Our lives and daily cycles are regulated by the Sun, but the solar day does not have a constant length because the apparent motion of the Sun on the celestial sphere is not uniform. This is due to the ellipticity of the Earth's orbit around the Sun and to the fact that the equatorial plane and the ecliptic plane do not coincide.

For this reason, the concept of the *mean Sun* was introduced. By definition, it moves at a uniform angular velocity (along the celestial equator) and transits the meridian every exact 24 hours.

Mean solar time refers to the fictitious observation of the mean Sun, *apparent solar time* to the real observation of the true Sun, and *sidereal time* to the real observation of a star or the fictitious observation of the Vernal Point (First Point of Aries).

Greenwich Mean Time (GMT) is a time standard based on the hour angle of the mean Sun at the Greenwich meridian, which was used as the reference for civil time worldwide until 1972. Noon GMT (12:00) corresponds to the transit of the mean Sun at the Greenwich meridian. When the meridian passing through the Royal Observatory in England was conventionally designated as longitude 0° (the prime meridian), the corresponding antimeridian on the opposite side of the Earth, located in the middle of the Pacific Ocean, was chosen as the 0-hour reference (the International Date Line), where the practical implications could be more easily managed.

Following the refinement of atomic clocks and precise measurements of Earth's rotation, GMT was replaced in 1972 by the current universal time scales, specifically Coordinated Universal Time (UTC). Terrestrial Time (TT), used in the file *MINDIST.DAT* of the Solex software and in astronomy for orbital and ephemeris calculations involving geocentric computations, differs from UTC by only a few seconds.

The longitude of a location is the spherical angle between the local meridian and the prime meridian (0°) passing through Greenwich. The local time at which the Sun transits the meridian of a given location (conjoined with the Moon in the specific case addressed here) is calculated based on the longitude offset from the prime meridian.

Each degree of longitude corresponds to 4 minutes of time difference relative to the Greenwich meridian. Consequently, the +14° meridian, which passes through the island of Procida west of the Campi Flegrei, corresponds to 11:04:00.

In this context, the Sun (together with the Moon, in the specific case under consideration) transits between 10:20:00 and 11:56:00 UTC across the Central European meridians spanning from 25° to 1° longitude. In this study, solar ephemerides are evaluated to determine the positions and syzygial times of the Moon, which necessarily coincide with those of the Sun, since the latter is always in conjunction with the Earth's satellite during New Moon culminations in Right Ascension.

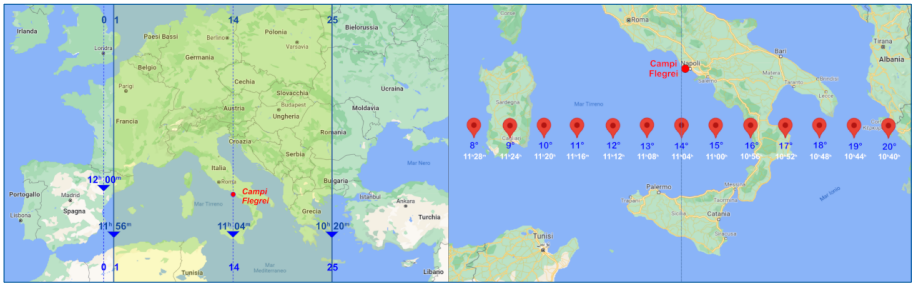

Fig. 26 Longitudes and corresponding UTC solar transit times at the meridian (Map data ©2025 Google).

By isolating the Moon–Sun conjunctions in right ascension that fall within the TT interval 10:20:00–11:56:00, the Central European New Moons (Moon+Sun) are obtained, orbiting over Italy (with partial inclusion of France and Greece).

The transit of the true Sun across the local meridian does not occur exactly every 24 hours but varies due to both the non-uniform velocity of the Earth in its orbit around the Sun and the obliquity of the

ecliptic plane. The combined effect of these two factors produces a complex variation known as the *Equation of Time (e)*. The time difference between the meridian transits of the true Sun and the mean Sun is expressed by the Equation of Time: it is positive when the true Sun is ahead and negative when the true Sun lags behind. This difference can be calculated as a function of the mean longitude of the Sun, i.e., theoretically.
The actual time of the Sun's transit at the local meridian is obtained by applying this variation: Apparent solar time = Mean solar time + e.
Accordingly, the times of the 25 Moon–Sun conjunctions (Fig. 14), here referred to as MNMs, should ideally be corrected using the Equation of Time. However, its maximum adjustment of ±15 minutes does not substantially affect the results shown in the graphical elaborations presented in this study.

2.5.2 Calculation procedures

To identify Moon–Sun conjunctions over the past 2101 years, the software Solex 12.1.01 (Solex, High Precision Ephemerides by Numerical Integration) was used. This is a celestial mechanics application with a precision equivalent to the online ephemerides system NASA/JPL Horizons.The alphanumeric coordinate files printed to file are available on Google Drive [14]
The computation of Moon–Sun conjunctions in right ascension for the period 0–2100 (produced in alphanumeric format and stored in the file MINDIST.DAT, which also served as the data source for Tabs 1–4) was performed using the following commands:

```
        Starting Solex
Enter   Continue
8       DE4068, no aster.
0       Jump to date
null    Step of 1 day
Off     Ensure that the reference frame is Geocentric Equatorial,
        i.e., with the following states set to Off:
        (O) Orthogonal, (H) Heliocentric,
        (T) Topocentric, (E) Ecliptic, (Z) Horizontal
Y       Cl. Approaches, Close approaches
E       Moon-Sun, compute superior Moon-Sun conjunctions
10/C    Maximum angular distance / Right Ascension conjunction
Y       Proceed
2101    Compute until the beginning of the year 2101
```

The calculation of Sun–Jupiter conjunctions in right ascension, with a minimum angular distance of 0.2°, occurring in the astronomical period 0–2100, was performed using the SOLEX software, which returned the data in alphanumeric format in the file MINDIST.DAT (the source of the data for Table 4), through the commands:

```
        Starting Solex
Enter   Continue
Enter   Continue
8       DE4068, no aster.
0       Jump to date
null    Step of 1 day
Off     Ensure that the reference frame is Geocentric Equatorial,
        i.e., with the following states set to Off:
        (O) Orthogonal, (H) Heliocentric,
        (T) Topocentric, (E) Ecliptic, (Z) Horizontal
/       Hide planets
Z       Hide all celestial bodies
0       Select the Sun
5       Select Jupiter
ESC     End, Exit
Y       Cl. Approaches, Close approaches
A       Angular, Angular distance
0-5     Select Sun and Jupiter, or All with -1
0.2/C   Maximum angular distance / Right Ascension conjunction
Y       Proceed
2101    Compute until the beginning of the year 2101
```

3 Conclusions

The analysis highlights a systematic correlation between ground uplift and subsidence and periods characterized by lunar culminations above or below 75°. This relationship is intrinsically linked to a periodicity consistent with what has already been reported in previous studies [7].
The observed discrepancies were interpreted through three distinct approaches, all based on the analysis of lunar orbital parameters and high-precision geometric modeling. Overall, the data reveal significant temporal correlations between specific geometric configurations of the three main external gravitational sources and the geophysical phenomena recorded along the Campi Flegrei–Vesuvio volcanic arc.
The evidence of this correlation suggests that the particular caldera morphology (broad, shallow, and not entirely overlain by volcanic reliefs) and the peculiar geodynamic setting of Italy configure a system more sensitive to cumulative harmonic stresses of tidal origin. In different geodynamic contexts, such effects tend to spread over much wider spatial scales, making them less discernible. However, this specificity may limit the possibility of generalizing the results, restricting the validity of the identified relationships to the study area. The Italian geodynamic framework, characterized by a high concentration of isolated volcanic activity compared to the surrounding European regions, seems to favor the observation of stronger correlations between the peaks of lunar, terrestrial, and solar interactions along the peninsula's meridians.
In summary, Phlegraean bradyseism exhibits a periodic regularity in its multi-year uplift and subsidence cycles, modulated by the height of lunar transit; meanwhile, sudden geophysical phenomena—such as major earthquakes and rapid uplifts—appear to be associated with transient gravitational configurations, marked by alignments among the three most attractive external celestial bodies.

4 References

[1] Pappalardo, L., Mastrolorenzo, G. Rapid differentiation in a sill-like magma reservoir: a case study from the campi flegrei caldera. Sci Rep 2, 712 (2012). https://doi.org/10.1038/srep00712

[2] E. Guidoboni, Pozzuoli terremoti e fenomeni vulcanici nel lungo periodo, a cura di AISI-Associazione Italiana di Storia dell'Ingegneria VIII Convegno di Storia dell'Ingegneria, da Gli Speciali de Il Giornale dell'Ingegnere, Gli Speciali de Il Giornale dell'Ingegnere

[3] D'Auria, L., Pepe, S., Castaldo, R. et al. Magma injection beneath the urban area of Naples: a new mechanism for the 2012–2013 volcanic unrest at Campi Flegrei caldera. Sci Rep 5, 13100 (2015). https://doi.org/10.1038/srep13100

[4] F. Di Luccio, G. Chiodini, S. Caliro, C. Cardellini, G. Ventura, (2018), Seismic signature of active intrusions in mountain chains. Science Advances, 3 Jan 2018,Vol. 4, Issue 1, doi: 10.1126/sciadv.1701825

[5] D. Zaccagnino, F. Vespe, C. Doglioni, (2020), Tidal modulation of plate motions. Earth-Science Reviews Volume 205, June 2020, 103179 doi:10.1016/j.earscirev.2020.103179

[6] Ide, S., Yabe, S. & Tanaka, Y. (2016), Earthquake potential revealed by tidal influence on earthquake size–frequency statistics. Nature Geosci 9, 834–837. https://doi.org/10.1038/ngeo2796

[7] Lambert S and Sottili G (2023) Possible role of tidal and rotational forcing on bradyseismic crises and volcanic unrest in the Campi Flegrei and Somma–Vesuvius areas. Front. Earth Sci. 11:1060434. doi: 10.3389/feart.2023.1060434

[8] Mario Baratta (1901) I terremoti d'Italia, Fratelli Bocca Editori Torino

[9] Del Gaudio et al. (2010) The bradyseismic deformation curve is taken, Journal of Volcanology and Geothermal Research, 195

[10] Dumont S, de Bremond d'Ars J, Boulé J-B, Courtillot V, Gèze M, Gibert D, Kossobokov V, Le Mouël J-L, Lopes F, Neves MC, Silveira G, Petrosino S and Zuddas P (2025) On a planetary forcing of global

seismicity. Front. Earth Sci. 13:1587650. doi: 10.3389/feart.2025.1587650

[11] Guidoboni, E., Ciuccarelli, C., (2011), The Campi Flegrei caldera: historical revision and new data on seismic crises, bradyseisms, the Monte Nuovo eruption and ensuing earthquakes (twelfth century 1582 ad). Bull Volcanol 73, 655–677 (2011). https://doi.org/10.1007/s00445-010-0430-3

[12] R. Scandone, J. D'Amato e L. Giacomelli, (2010), The relevance of the 1198 eruption of Solfatara in the Phlegraean Fields (Campi Flegrei) as revealed by medieval manuscripts and historical sources, Journal of Volcanology and Geothermal Research Volume 189, Issues 1–2, 1 January 2010, Pages 202-206

[13] A high-resolution version of the graphic is available as supplementary material on Google Drive: Synchronization of Harmonics and Seismic Storms.pdf

[14] A 1905 2100 Topocentric Coordinates of Pozzuoli ----- (1 980 000 Rows).txt (1.6 Gbytes)
B 0000-2100 Geocentric Moon-Sun Conjunctions in RA ----- (25 986 Rows).txt
B 1905 2044 Geocentric Moon-Sun Conjunctions in RA with asterisks ----- (1734 Rows).txt
C 1905-2100 Major Moons ----- (30 Rows).txt
D 0000-2025 Extreme Moons ----- (14 Rows - Tab 1) .txt
E 0000-2100 Central European Solstitial Geocentric Moon-Sun Conjunctions in RA ----- (27 Rows - Tab. 2).txt
F 0000-2100 Geocentric Sun-Jupiter Conjunctions in RA Ang. Dist. 0.2°----- (212 Rows).txt
G 0000-2100 Geocentric Sun-Jupiter Conjunctions in RA Ang. Dist. 1.10° ----- (1373 Rows).txt

5 Keywords

bradyseism, volcanic unrest, Campi Flegrei caldera, Vesuvio, Phlegraean Fields, Vesuvius, tides, tidal modulation, tidal tilting, crustal response to earth tides, seismic and volcanic activity, Earth–Moon–Sun–Jupiter alignment